

MAR 1 1972

MAR 14 1972

cy.2



VELOCITY MEASUREMENTS IN AERODYNAMIC WIND TUNNEL (1T) USING A LASER DOPPLER VELOCIMETER

F. H. Smith, A. E. Lennert, and J. O. Hornkohl
ARO, Inc.

February 1972

Approved for public release; distribution unlimited.

**ARNOLD ENGINEERING DEVELOPMENT CENTER
AIR FORCE SYSTEMS COMMAND
ARNOLD AIR FORCE STATION, TENNESSEE**

PROPERTY OF U S AIR FORCE
AEDC LIBRARY
F40600-72-C-0003

NOTICES

When U. S. Government drawings, specifications, or other data are used for any purpose other than a definitely related Government procurement operation, the Government thereby incurs no responsibility nor any obligation whatsoever, and the fact that the Government may have formulated, furnished, or in any way supplied the said drawings, specifications, or other data, is not to be regarded by implication or otherwise, or in any manner licensing the holder or any other person or corporation, or conveying any rights or permission to manufacture, use, or sell any patented invention that may in any way be related thereto.

Qualified users may obtain copies of this report from the Defense Documentation Center.

References to named commercial products in this report are not to be considered in any sense as an endorsement of the product by the United States Air Force or the Government.

VELOCITY MEASUREMENTS IN
AERODYNAMIC WIND TUNNEL (1T)
USING A LASER DOPPLER VELOCIMETER

F. H. Smith, A. E. Lennert, and J. O. Hornkohl
ARO, Inc.

Approved for public release: distribution unlimited.

FOREWORD

The test reported herein was sponsored by Headquarters, Arnold Engineering Development Center (AEDC), Air Force Systems Command (AFSC), under Program Element 64719F.

The work was done by ARO, Inc. (a subsidiary of Sverdrup & Parcel and Associates, Inc.), contract operator of AEDC under Contract F40600-72-C-0003. The ARO project number was BC5119, and the manuscript was submitted for publication on June 1, 1971.

The authors wish to acknowledge R. E. Dix, Propulsion Wind Tunnel Facility, and D. B. Brayton and H. T. Kalb, Technical Staff, in assisting with the work reported herein.

This technical report has been reviewed and is approved.

David G. Francis
Captain, USAF
Research and Development
Division
Directorate of Technology

R. O. Dietz
Acting Director
Directorate of Technology

ABSTRACT

This report describes the application of a laser Doppler velocimeter (LDV) in a transonic wind tunnel. The LDV, an in-house-developed instrument, measured two velocity components using the dual scatter principle. The flow was not seeded for this test, and the output data was processed by a special data processor developed at AEDC. The velocity data and flow angularity are presented for five Mach numbers together with the velocities obtained using conventional wind-tunnel instrumentation.

CONTENTS

	<u>Page</u>
ABSTRACT	iii
I. INTRODUCTION	1
II. DESCRIPTION OF THE 1-FT WIND TUNNEL	1
III. LASER DOPPLER VELOCIMETER AND INSTRUMENTATION	2
IV. INSTALLATION AND TEST PROCEDURES	3
V. DATA REDUCTION	5
VI. RESULTS AND DISCUSSION	7
VII. SUMMARY OF RESULTS.	9
REFERENCES	10

APPENDIX ILLUSTRATIONS

Figure

1. The 1T, Two-Component, Dual Scatter LDV	13
2. 1T LDV Self-Aligning Optics	14
3. 1T LDV Input Optics Traverse.	15
4. 1T LDV Receiving Optics and Traverse	16
5. LDV Beam Orientation about Test Cell Centerline	17
6. LDV Signal Processing and Recording Equipment	18
7. Computer Printout of Input Data and Component Velocity.	19
8. Computer Printout with Input Data Limited to $\pm 2\sigma$ of Mean	19
9. Schematic of Test Section, PWT 1T Tunnel	20
10. Horizontal Velocity versus Axial Tunnel Position, M = 0.6	21
11. Horizontal Velocity versus Axial Tunnel Position, M = 0.8	22
12. Horizontal Velocity versus Transverse Position, M = 0.8	23
13. Horizontal Velocity versus Transverse Position, M = 1.0	24

<u>Figure</u>		<u>Page</u>
14.	Horizontal Velocity versus Transverse Position, M = 1.2	25
15.	Centerline Velocity, M = 1.5	26
16.	Flow Angularity versus Axial Position, M = 0.6	27
17.	Flow Angularity versus Axial Position, M = 0.8	28
18.	Flow Angularity versus Transverse Position, M = 0.8	29
19.	Flow Angularity versus Transverse Position, M = 1.0	30
20.	Flow Angularity versus Transverse Position, M = 1.2	31
21.	Flow Angularity at Tunnel Centerline, M = 1.5	32
22.	Nondimensionalized Velocities versus Tunnel Position, M = 0.6	33
23.	Nondimensionalized Velocities versus Tunnel Position, and M = 0.8	34
24.	Nondimensionalized Velocities versus Tunnel Position, M = 0.8	35
25.	Nondimensionalized Velocities versus Tunnel Position, M = 1.0	36
26.	Nondimensionalized Velocities versus Tunnel Position, M = 1.2	37
27.	Nondimensionalized Velocities versus Tunnel Position, M = 1.5	38

SECTION I INTRODUCTION

The application of the laser Doppler velocimeter (LDV) for making velocity measurements of fluid flows has several distinct advantages over conventional measurement techniques. It has the ability to make measurements without perturbing the flow and also to make point velocity measurements in small or inaccessible areas. There have been minor drawbacks to the application of the LDV to actual wind-tunnel measurements. First, there was the necessity to seed the flow being measured, and the time required to make a velocity measurement using a spectrum analyzer for the frequency readout instrumentation was exceedingly lengthy. These drawbacks were recognized (Ref. 1), and with extensive development work have been eliminated. In September 1970 the USAF at AEDC requested a test be performed to demonstrate the following LDV capabilities:

1. Calibration measurements were to be made in a transonic wind tunnel covering both subsonic and supersonic flows.
2. Artificial seeding of the airflow would not be allowed in performing the measurements.
3. A two-component, dual scatter LDV was to be used.
4. Automatic data acquisition electronics would be employed.

The test was successful in meeting all the requirements, and this report presents the LDV results together with the wind-tunnel calibration velocity data for comparison.

SECTION II DESCRIPTION OF THE 1-FT WIND TUNNEL

The Aerodynamic Wind Tunnel (1T) in the Propulsion Wind Tunnel Facility (PWT) is a continuous flow, nonreturn design (Ref. 2). It is powered by a 3000-hp, constant-speed motor driving a single-stage compressor which delivers the air into a stilling chamber having bypass and recirculation circuits. The tunnel nozzle has rigid, paralleled side plates and flexible top and bottom plates which can be adjusted to obtain supersonic velocities. The tunnel is normally operated over a Mach number range from 0.20 to 1.50. It has a test section 12 in.

square in cross section and 37.5 in. long which is enclosed in a plenum chamber connected to a steam ejector evacuation system. The test section walls are normally perforated to allow partial pumpout of the test section through the plenum chamber; however, for this test the side walls were replaced with walls having optical glass inserts. These inserts are 9 in. high and 11-1/2 in. long, extending from tunnel station (TS) 14.8 to 26.3 and centered on the tunnel horizontal centerline. The plenum chamber walls have optical quality inserts which superpose the test section inserts. No models or stings were present in the tunnel during this test.

SECTION III LASER DOPPLER VELOCIMETER AND INSTRUMENTATION

The Laser Doppler Velocimeter (LDV) used for this test was a two-component, dual-scatter unit used in the forward-scattering mode. The size and construction of the 1T wind tunnel made it necessary to assemble the LDV as two independent packages (Fig. 1, Appendix). The laser, a Spectra-Physics Model 140 argon laser with a nominal power output of 0.75 watts at a 4880-Å wavelength in the TEM₀₀ mode, and the input optics consisting of the beam expanding and collimating lenses, self-aligning beamsplitters (Refs. 3 and 4), polarization rotators, and the 3-in. -diameter, 36-in. focal length focusing lens comprised the input package. The laser, beam expanding and collimating lenses, and the self-aligning beamsplitters were remotely located from the wind tunnel (Fig. 3). The polarization rotators and the focusing lens were mounted on an x-y traverse which allowed measurements to be made axially and transversely through the wind tunnel test section. The beams were brought up from the beam-splitters to the traverse by first surface dielectric mirrors.

The probe volume formed by the intersection of the input beams is an ellipsoid and had characteristic dimensions of 0.094 in. in length and 0.011 in. for the major diameter. The volume of the ellipsoid was 7.42×10^{-5} cc.

The output or receiving optics which were located on the opposite side of the wind tunnel (Fig. 4) consisted of two 6-in. -diam, 30-in. focal length lenses which collimated and focused the scattered light from the probe volume onto a pinhole aperture, a collimating lens, a polarization separation prism, and two photomultiplier (PM) tubes. The pinhole aperture and the collimating lens were mounted on a precision micro-traverse. All of these optics were mounted on an x-y traverse which matched the movement of the input optics traverse.

Selective light polarization was used to discriminate between the two velocity components. The beam splitters divided the input laser beam into three path-length-compensated beams with intensity levels of 25, 50, and 25 percent of the input beam (Fig. 5). These three beams formed a right triangle with the most intense (50 percent) beam at the vertex of the triangle. The input polarization rotators rotated the polarization plane of the 50-percent beam by 45 deg and one of the 25-percent beams by 90 deg. This rotation cross polarized the two velocity component measuring beams (i. e., the polarization plane for one velocity component was made perpendicular to the polarization plane of the second velocity component) and substantially reduced the mutual interference or cross-talk between them. The polarization separation prism (Glan-Foucault air-spaced type) in the receiving optics was properly rotated about its axis to transmit the polarization of one velocity component and internally reflect the polarization of the other component. The PM tube for the transmitted component was mounted directly behind the prism. The PM tube for the reflected component was mounted to one side and the polarized, scattered light directed to it with a first surface mirror.

The PM tubes were RCA Model 8644 with external resistor bias networks installed. The PM tube output was connected in parallel with a Tektronix Model 585 oscilloscope and the Doppler Data Processor* (DDP) (Ref. 1). This is an in-house developed instrument which determines the period of the Doppler signal produced by a particle crossing the probe volume. The DDP is a plug-in module used in conjunction with a modified Hewlett-Packard Model 5245M counter. The frequency range of the DDP used in this test was 1 to 50 MHz. The period of the Doppler frequency is displayed on the counter and printed out by a Hewlett-Packard Model 5050A digital line printer. The limit of this printer is 20 lines/sec which fixed the maximum rate of data acquisition. A block diagram of the signal processing and recording equipment is shown in Fig. 6.

SECTION IV INSTALLATION AND TEST PROCEDURES

The installation of the LDV in the 1T tunnel test area required two alignments; the mechanical alignment of the two traverses and the alignment of the optics. The mechanical alignment consisted of locating the

*Patent pending

traverse platforms relative to the test section windows so that the movement of the traverses encompassed the test section windows, then leveling and aligning them so that a point on the traverses remained equidistant from the test section windows during horizontal traversing and perpendicular to the windows during transverse traversing. The input optics mirrors were aligned so the point of intersection (probe volume) of the three input beams remained in a horizontal plane during traversing. The probe volume was physically located on the vertical centerline ($Y = 0$) of the test section by positioning the input traverse and the input focusing lens. Prior to installing the receiving optics, the input beams were allowed to expand from their focal intersection onto the test area wall approximately 30 ft away. Here, they were precisely located relative to each other. This allowed the determination of the angle between the beam pairs, their orientation relative to the test section centerline, and the angle θ for each of the beam pairs. Initially, the common angle between the beams was $88^{\circ}55'$, with one beam oriented $30^{\circ}58'$ above the test section centerline and the other $57^{\circ}57'$ below the centerline (Fig. 5a). The subsequent orientation had one beam at $44^{\circ}38'$ above the centerline and the other at $44^{\circ}17'$ below it. The included angle between them remained $88^{\circ}55'$ (Fig. 5b). The receiving optics were installed, and the direct beams passing through the probe volume were blocked at the output collimating lens. This reduced the background noise level of the PM tubes caused by extraneous scattering from these beams. The focusing lens, aperture, the polarization separator, and the PM tubes were then aligned with the probe volume. This alignment was checked to verify that it was maintained when traversing both the input and receiving optics.

The test requirements specified data to be taken on the test section centerline at Mach numbers 0.6, 0.8, 1.0, and 1.2 with traverses to be made across the test section (y) if there was time available. The measurements were made in order of increasing Mach number. Since there was no artificial seeding of the flow, the time required to make a velocity measurement at one location varied from a few seconds to several minutes, depending upon the time average of the particulate concentration at the measurement location. An attempt was made to obtain a sufficient, and approximately equal, number of data points at each measurement location so that a good statistical sample of the velocity distribution could be obtained. The sampling time at each location was further increased since only one DDP unit was available for use. This necessitated connecting it to a PM tube and taking data on one component then disconnecting and connecting to the other PM tube to obtain data on the second component. Alignment was verified at each position during the traverses.

When the data at Mach number 1.2 were completed, there was a limited amount of tunnel time remaining. Since all specified data had been taken, the tunnel was operated at Mach number 1.5 and the time was used to record velocities at a single centerline location. During the time the LDV measurements were being made, conventional wind-tunnel pressures and temperatures were recorded by PWT personnel and using previous tunnel calibrations determined the free-stream velocity for comparison with the LDV data. Although conventional velocity data were not taken for all LDV data points, a sufficient number were obtained to give a comprehensive comparison.

SECTION V DATA REDUCTION

The processing of LDV particle burst data requires a terminology explanation to properly define it. A data point refers to the Doppler frequency information obtained from a single particle passing through the focal volume. A component velocity is the velocity of a single component of a multi-component LDV which is determined from many individual data points. The velocity refers to the magnitude of the velocity vector at some particular flow angle, which is determined from the two component velocities at some particular spatial location in the test section.

The 1T tunnel test involved 6729 individual data points. They ranged in number from six to as high as 384 for an individual velocity component with an average number of 104 data points per component.

The output of the DDP is the period of the Doppler frequency in nanoseconds and was printed in digital form on a paper tape. Since many of these data points are used to determine a single velocity component, a computer program was written to evaluate the data. The program determined the arithmetic mean period and the RMS variation about the mean for each group of component data. Nine statistical bands were then established, each 1/4 standard deviation (Ref. 5) ($\sigma/4$) wide around the mean, and the percentage of the velocities that fell within these bands was determined. Finally, a Gaussian distribution curve was established,

$$G(v) = \frac{1}{\sigma\sqrt{2\pi}} e^{-\left(\frac{v - \bar{v}}{2\sigma^2}\right)^2}$$

where v is the velocity at a point and \bar{v} is the average velocity of the stream. The number of data points that fell under this curve was determined. A typical set of data from the program is shown in Fig. 7. The Gaussian distribution gives an indication of the validity of the statistical sample. If an infinite number of data points were taken, the distribution of the data should fall under the resulting Gaussian curve. At the completion of this calculation, the period data were recycled by the computer, and based upon the RMS (σ) variation determined from the first cycle, all data points whose value was more than two standard deviations (2σ) above or below the mean period were eliminated. This procedure eliminated any obviously scattered data points and a new mean period, an RMS variation about the mean, new statistical distribution bands, and the Gaussian distribution curve based on this data were recalculated by the computer. The results of this procedure applied to the data of Fig. 7 are shown in Fig. 8. The number of data points that fell more than 2σ beyond the mean was, on the average, four percent of the total. The mean period and the RMS period values of the component velocity were converted into mean velocity and an RMS variation in fps, which was referred to the horizontal axis of the wind-tunnel test section.

The magnitudes of the velocities of the two components for $M \geq 0.8$ should have been identical since the beam pairs were set at ~ 45 deg to the test section axis, and the velocity was assumed to be parallel to the axis. However, in no case was this true. This led to the conclusion that the velocity at the point of measurement was not parallel with the tunnel axis. The two components were therefore solved simultaneously to determine the magnitude and angle of the velocity vector with respect to the horizontal axis of the tunnel test section. The RMS or standard deviation of this velocity was statistically determined (Ref. 6). This technique demonstrates that when an unknown is measured by two methods, each having standard deviations σ_i , $i = 1, 2$, the standard deviation of the resulting combination of the two can be determined by the relationship

$$\sigma \bar{v} = \sqrt{\frac{\sigma_1^2 + (\sigma_1/\sigma_2)^4 \sigma_2^2}{(1 + (\sigma_1/\sigma_2)^2)^2}}$$

where a weighted average of the standard deviations of the two component velocities is used to obtain the deviation of the velocity vector.

The reduction of the individual data points to determine the component velocities, RMS and distribution data, was done on the IBM 360-50 computer. The simultaneous solution of the components to determine velocities, flow angles, and the velocity RMS deviation were accomplished using a Wang Loci II computer.

SECTION VI RESULTS AND DISCUSSION

The coordinate convention and the area of measurement are shown in Fig. 9. The data are presented by Mach number and position. Data taken for $M = 0.6$ are shown in Fig. 10. These data fall generally from 710 to 715 fps. Six PWT data points are also shown that were taken simultaneously with their corresponding LDV point. These points were based on the latest tunnel calibrations and were corrected for axial Mach number distribution in the data reduction process. The variation in velocity - or error estimate - shown with the PWT data is a constant for any Mach number since it is primarily a function of instrument precision and reading accuracy. The LDV RMS and the PWT estimated error values overlap each other at all points in Fig. 10, indicating a very good correlation between the data at this Mach number.

Two traverses, axial and transverse, were made at a Mach number of 0.8. Figure 11 shows the data for the axial (x) traverse. These data were taken in increments of two inches. The LDV data are grouped around $925 \text{ fps} \pm 3 \text{ fps}$. The RMS and the PWT estimated error limits overlap each other only on the first two points. The PWT velocity adjusted for axial position drops off about 7 fps from the initial to the final point, which is much more pronounced than in the $M = 0.6$ traverse where it was practically constant. The transverse traverse at $M = 0.8$ is shown in Fig. 12. This and the succeeding traverses were made at Tunnel Station (TS) = 20.55 in. The LDV data showed a decrease in velocity from 935 to approximately 925 fps across the test section from the left to right looking upstream. The PWT velocity was 914 fps and is shown at the centerline position only since no correction could be made for transverse position. The separation between them was approximately 4 fps.

A transverse traverse was made at $M = 1.0$. The LDV velocity spread (Fig. 13) was between 1149 and 1156 fps. A very large RMS spread occurred at $y = 4 \text{ in.}$ This was because of large RMS deviations associated with the components at this location indicating that the particles being measured had widely fluctuating velocities. The PWT center-line velocity was 1135 fps. The LDV RMS limits only at the $y = 4\text{-in.}$ position approximated the PWT estimated error at the centerline. The transverse traverse at $M = 1.2$ (Fig. 14) showed a much greater variation in flow velocity across the test section. The estimated error limits of the PWT centerline measured velocity of 1322 fps was in good correlation with the LDV RMS spread except at the $y = -4 \text{ in.}$ position where the LDV measured velocity increased sharply

to 1349 fps. The LDV RMS values were approximately ± 10 fps for all data points. A single centerline data point (Fig. 15) was taken at $M = 1.5$. The discrepancy between LDV and PWT data was most pronounced at this Mach number, with the LDV measuring 1614 fps and PWT measuring 1571 fps. The LDV RMS remained about the same as on previous points, whereas the PWT estimated errors decreased as an inverse function of Mach number.

The data in Figs. 10 through 15 are for flow velocity magnitude only. The flow angularity for these data is shown in Figs. 16 through 21 and is plotted in degrees above or below the test section centerline as a function of location. Figure 16 shows the angularity for the $M = 0.6$ traverse. No data are shown at $TS = 19.55$ in. since only one component of velocity was measured and therefore no angularity could be determined. Likewise, the velocity at this location, shown in Fig. 10, was from one component. The flow angularity for the $M = 0.8$ axial traverse (Fig. 17) shows little correlation with the $M = 0.6$ traverse other than the flow angularity at $TS = 18.55$ in., which is -0.1 deg for both. The transverse traverses indicate the greatest flow angularity. Figure 18, for $M = 0.8$, shows an angularity of 0.58 deg at $y = 4$ in., with all the other data less than 0.25 deg. The angularity plots for $M = 1.0$ and $M = 1.2$ (Figs. 19 and 20) show characteristics similar to those in the $M = 0.8$ plot, not only in the large flow angle at $y = 4$ in., but also in the magnitudes and signs of the angles. The single measurement at $M = 1.5$ is shown in Fig. 21 and has a flow angle of 0.14 deg. The deviation of the angular measurements is shown plotted with the data. These angular deviations were a function of the RMS deviations of the component velocities used in the angularity calculations, and therefore varied rather widely as shown on Fig. 17. The flow angularity for $TS = 16.55$ was calculated to be -0.05 deg but the deviation was ± 0.25 deg, while at $TS = 20.55$ it was -0.21 deg with a deviation of ± 0.015 deg. Generally, the centerline data had the smallest angular deviations as indicated in Figs. 18, 19, and 21. The greatest deviation was ± 0.25 deg which occurred at $TS = 16.55$ on Fig. 17 and the smallest was 0.002 deg at $y = 0$ on Fig. 18.

Figures 22 through 27 illustrate the nondimensional velocity ratios. The axial traverses (Figs. 22 and 23) have data only where there were corresponding PWT data. All LDV velocities were normalized with the one centerline PWT velocity for the transverse traverses in Figs. 24 through 27. These curves illustrate the variation relative to the centerline velocity rather than at the actual position. All of the data had a variation less than 2.5 percent except for $M = 1.5$ where the variation was approximately 2.7 percent. One interesting fact is apparent: all of the LDV measured velocities were greater than the PWT-determined

velocities. No explanation is offered at this time for this result. On the contrary, one reasons that the particle velocity will lag the flow velocity by some small amount; however, this was not indicated.

SECTION VII SUMMARY OF RESULTS

The LDV successfully demonstrated several capabilities in this test that prior to this time were only known to be theoretically possible or were confirmed only in the laboratory. The first, and perhaps the most significant of these, was the ability to make velocity measurements with no artificial seeding of the flow, using only the natural contaminants present in the air.

The use of the DDP electronic data acquisition system showed that "on-line" velocity data can be easily, quickly, and accurately acquired and processed. The data can then be further processed, statistically analyzed, or examined at leisure. This is a significant improvement over previous techniques using spectrum analyzers which give an integrated average of the data over some finite time period.

The two-component LDV provided flow angularity data in a very rapid, straightforward way. The acquisition of both components yielded an average of flow velocity variations in both magnitude and direction at a point in the flow. With the inclusion of additional Doppler Data Processor systems in the near future, simultaneous acquisition of multicomponent data should be possible. This should be a valuable tool for the study of turbulence and turbulent fluctuations by providing a technique for a much more comprehensive understanding of the turbulent process.

Finally, the LDV has demonstrated the capability of making fast, accurate velocity measurements in a transonic wind tunnel under operational conditions. The full range of velocities was measured without modifying either the LDV optics or the data acquisition instrumentation. The traverses through the test section were accomplished without difficulty. Mechanical vibrations, present in every wind tunnel, presented no obstacle to the successful operation of the LDV.

REFERENCES

1. Lennert, A. E., Brayton, D. B., Crosswy, F. L., et al. "Summary Report of the Development of a Laser Velocimeter to be Used in AEDC Wind Tunnels." AEDC-TR-70-101 (AD871321), July 1970.
2. Test Facilities Handbook (Eighth Edition). "Propulsion Wind Tunnel Facility, Vol. 5." Arnold Engineering Development Center, December 1969.
3. Brayton, D. B. "A Simple Laser Doppler Shift Velocimeter with Self-Aligning Optics." Proceedings of the Electro-Optical Systems Design Conference, September 16-18, 1969. New York, N. Y.
4. Brayton, D. B. and Goethert, W. H. "A New Dual Scatter Laser, Doppler Shift Velocity Measuring Technique." Proceedings of the Sixteenth International ISA Aerospace Instrumentation Symposium, May 11-13, 1970.
5. Standard Handbook for Mechanical Engineers. Baumeister and Marks, Seventh Edition, pp. 17-25.
6. Beers, Y. "Introduction to the Theory of Error," Chapter VI, Section A. Addison-Wesley Publishing Company, Reading, Massachusetts, 1957.

**APPENDIX
ILLUSTRATIONS**

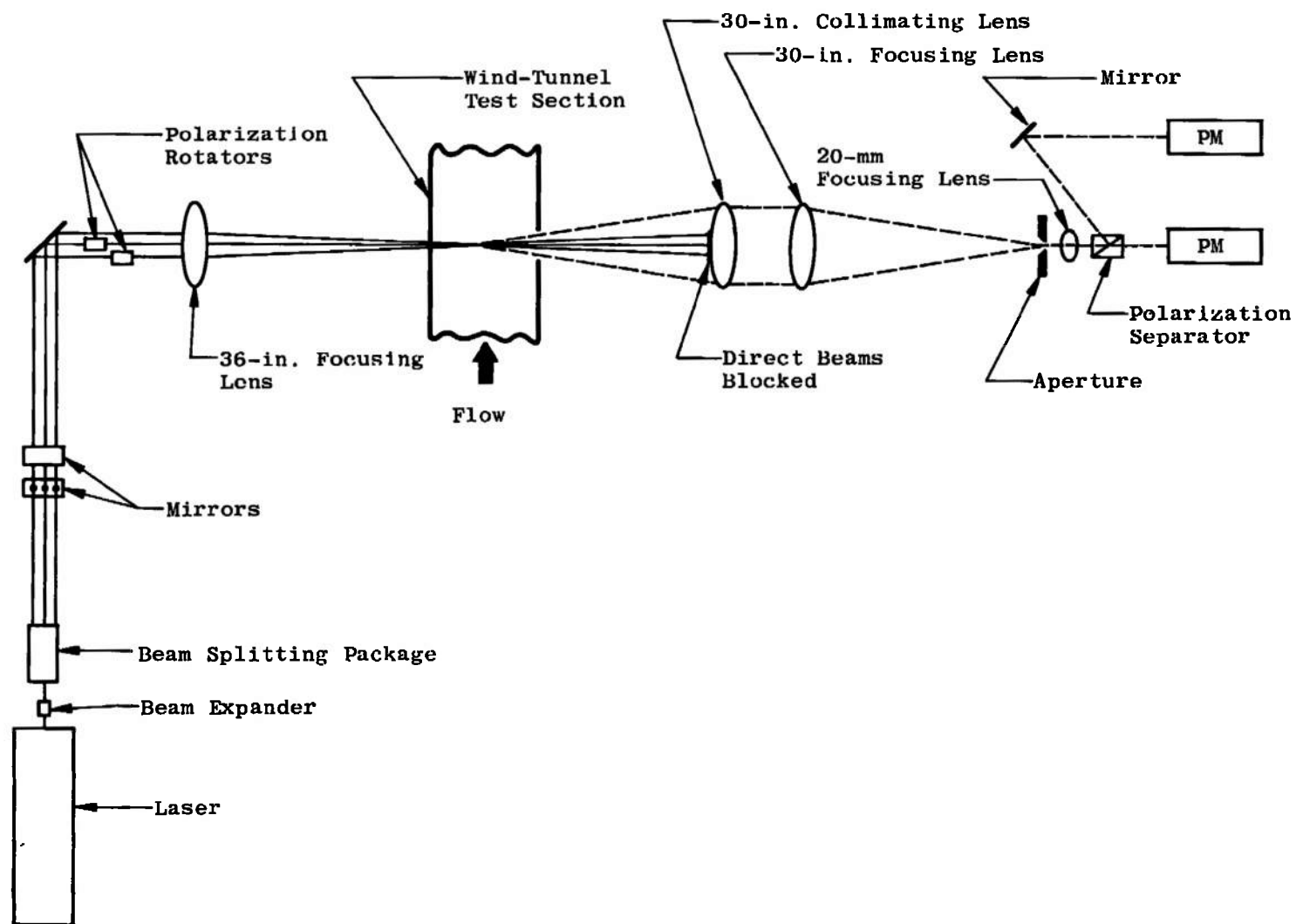


Fig. 1 The 1T, Two-Component, Dual Scatter LDV

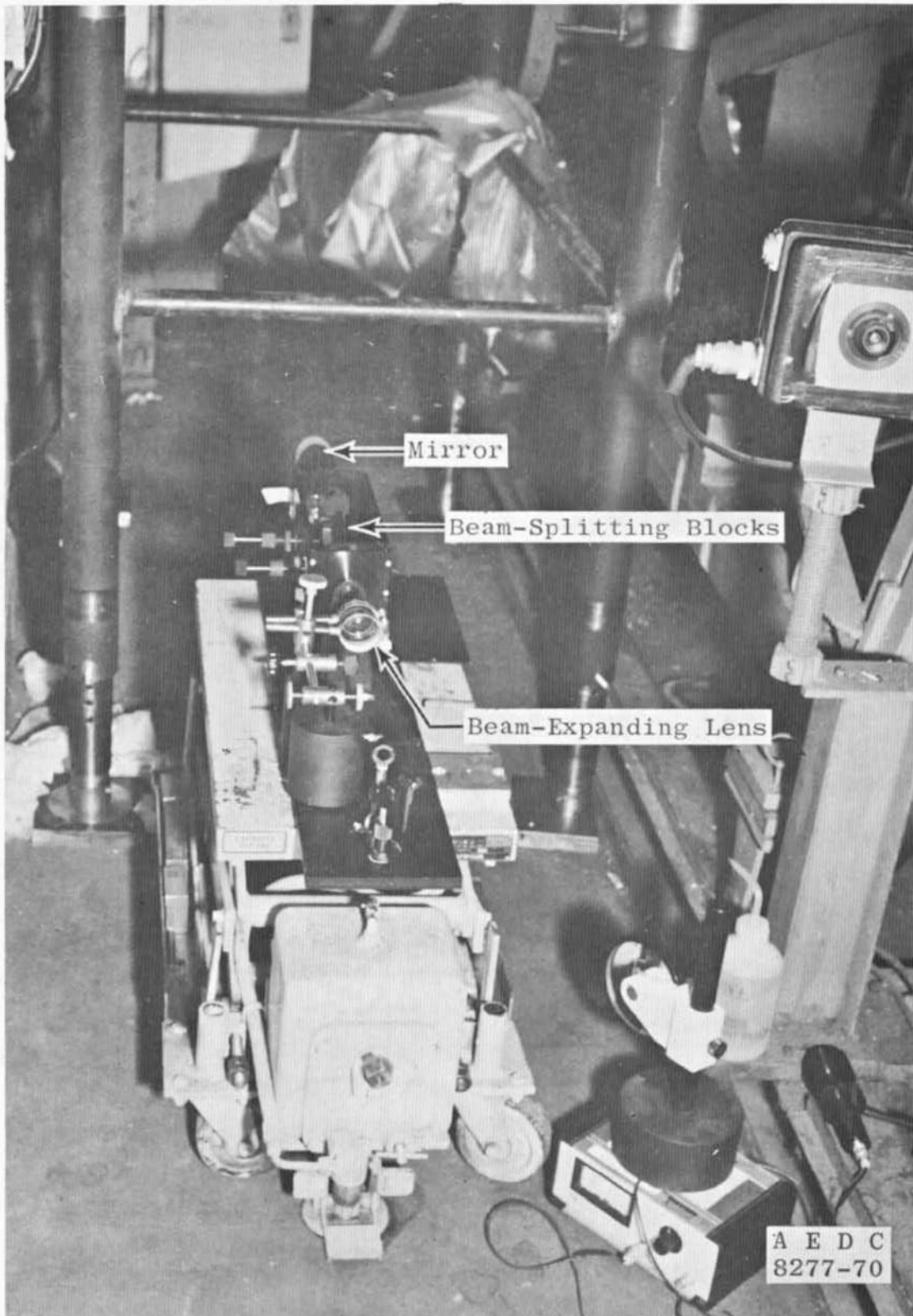


Fig. 2 1T LDV Self-Aligning Optics

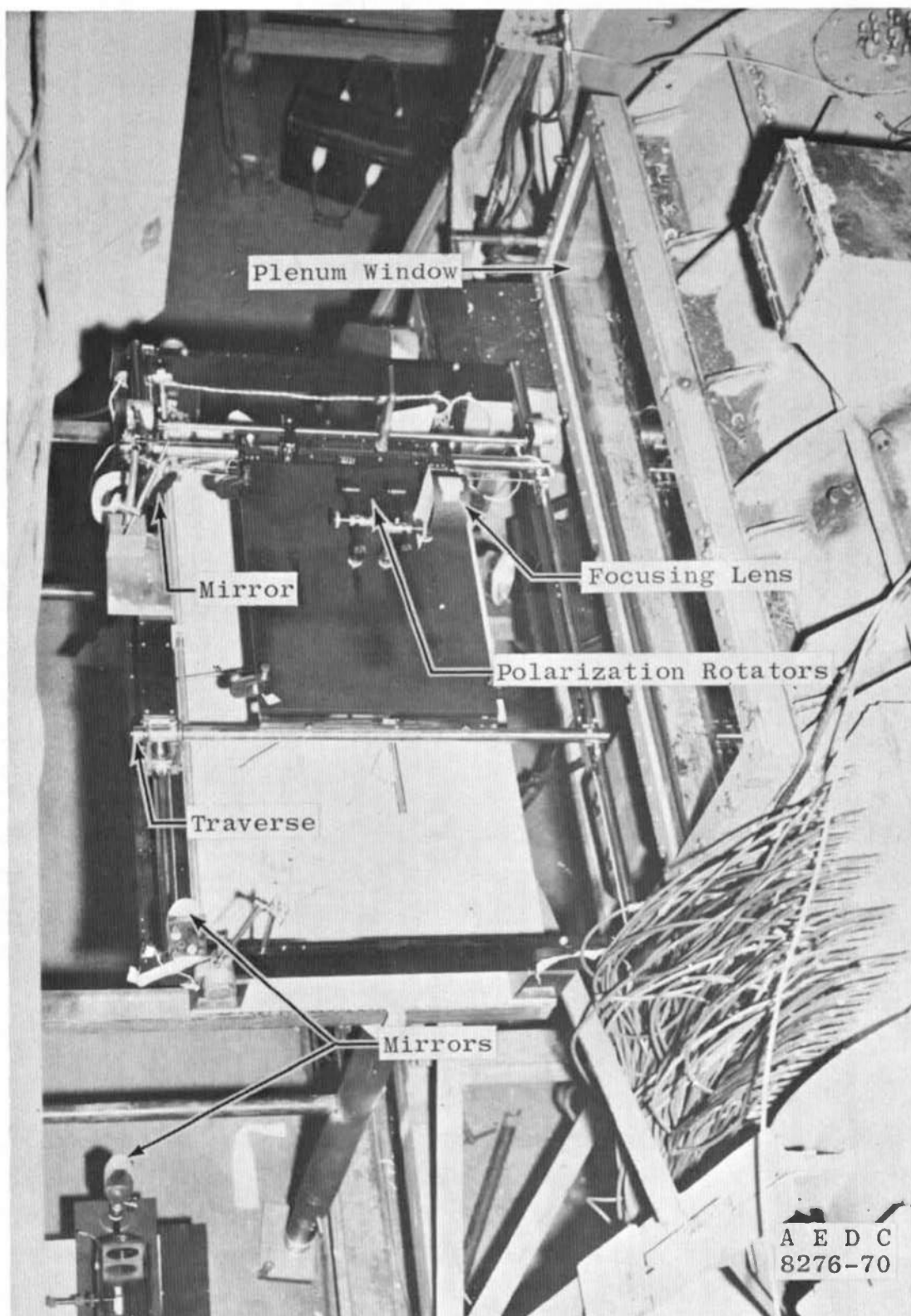


Fig. 3 1T LDV Input Optics Traverse

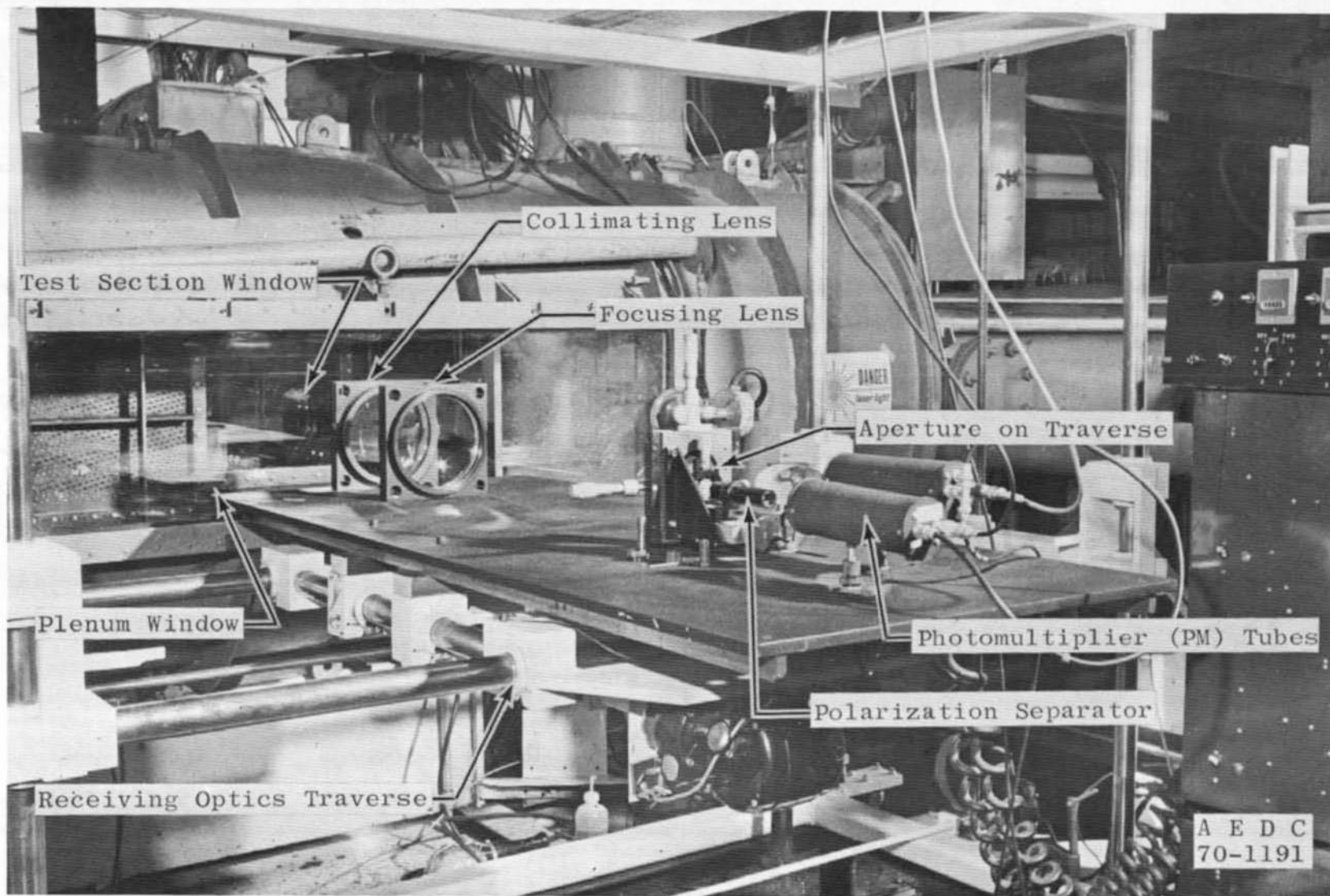
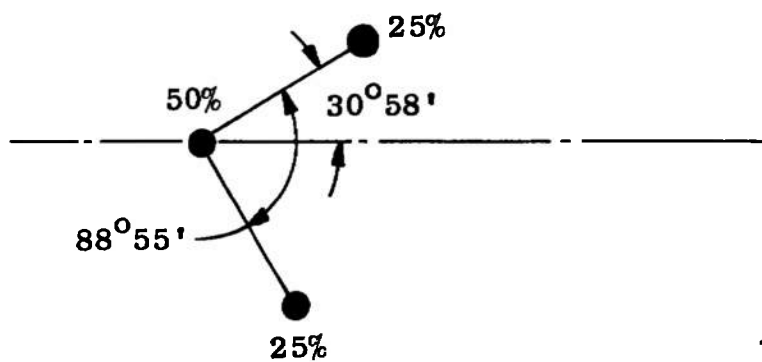
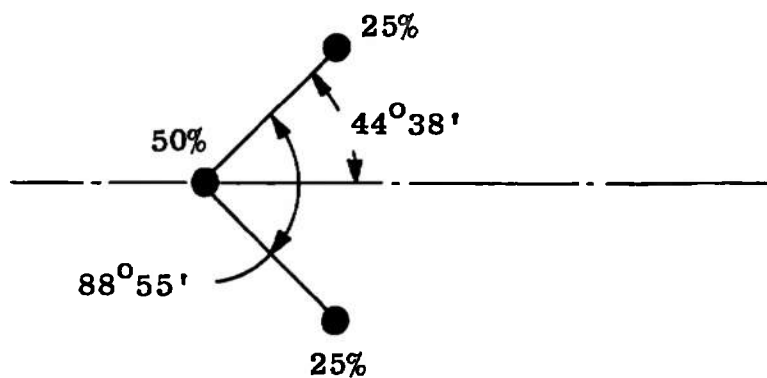


Fig. 4 1T LDV Receiving Optics and Traverse



a. Initial Orientation



b. Final Orientation

Fig. 5 LDV Beam Orientation about Test Cell Centerline

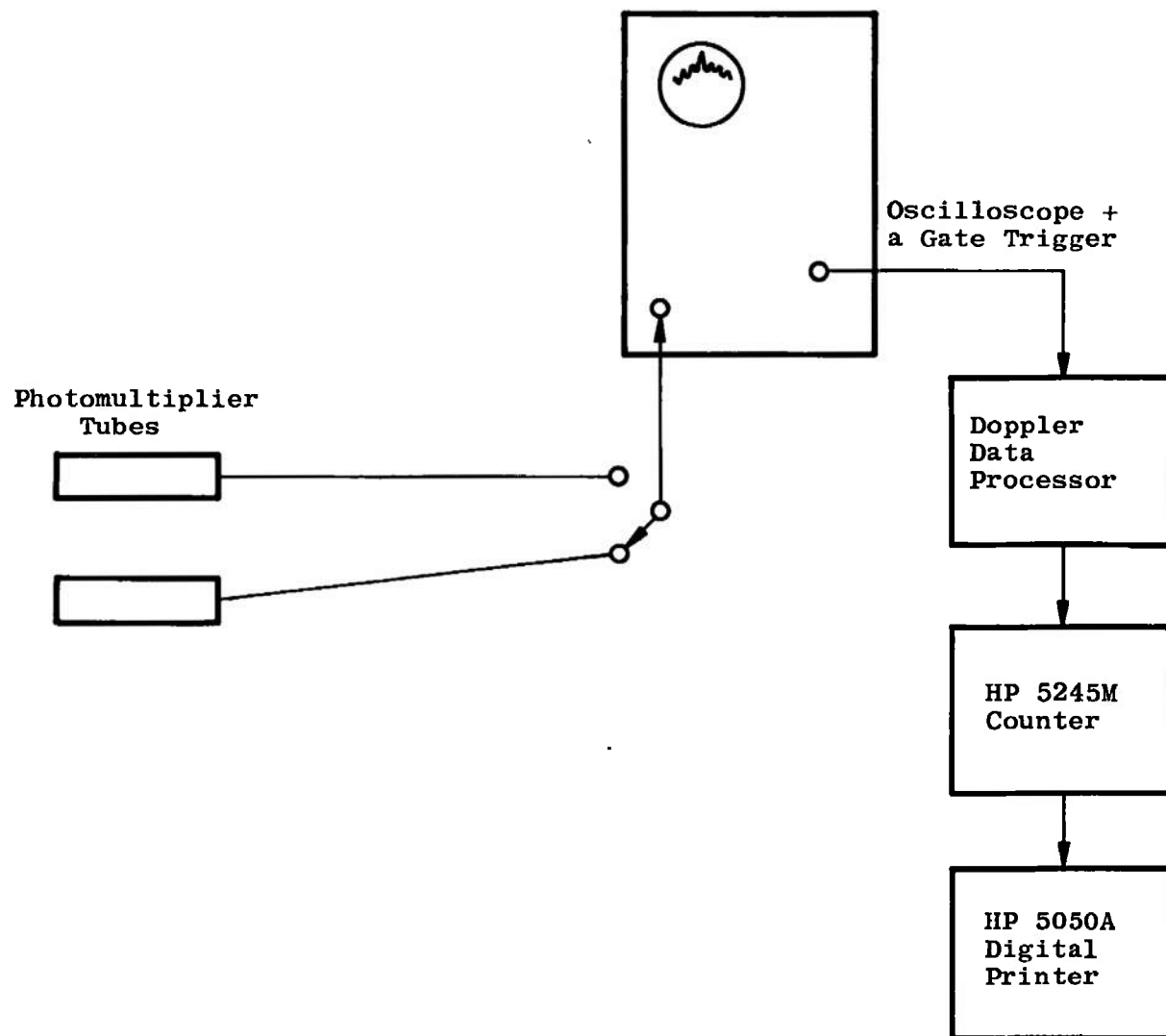


Fig. 6 LDV Signal Processing and Recording Equipment

X = 6.00 Y = 6.00 MACH 0.60 COMPONENT 1

DATA

```

104.72 107.94 109.97 107.53 107.11 106.23 109.36 108.12 106.17 108.86
107.70 110.59 107.28 106.88 106.28 106.76 106.34 107.49 108.40 107.32
106.89 109.31 108.02 107.94 107.27 106.39 108.21 108.42 107.30 107.19
107.98 108.37 108.80 108.52 107.24 106.32 109.69 107.28 108.27 107.22
108.31 106.72 107.28 108.85 109.49 108.17 107.58 105.46 108.52 108.95
107.51 110.60 107.91 108.13 106.58 107.83 108.39 107.24 108.23 110.08
108.75 105.95 107.77 107.11 107.45 107.57 107.42 108.62 106.59 107.33
107.16 108.64 109.10 107.63 107.65 108.44 108.78 109.69 107.72 107.32
105.50 105.31 106.66 107.30 104.37

```

AVERAGE PERIOD = 0.10771E 03 RMS = 0.12000E 01 = 0.11141E 01 PERCENT

AVERAGE VELOCITY = 0.71043E 03 +/- 0.79149E 01

POPULATION DENSITIES

-4	-3	-2	-1	0	+1	+2	+3	+4
0.0700	0.0471	0.2353	0.4235	0.4000	0.3529	0.2118	0.1176	0.0471

85 DATA PTS 81 PTS UNDER CURVE = 0.95 PERCENT

Fig. 7 Computer Printout of Input Data and Component Velocity

X = 6.00 Y = 6.00 MACH 0.60 COMPONENT 1

DATA

```

107.94 109.97 107.53 107.11 106.23 109.36 108.12 106.17 108.86 107.70
107.28 106.88 106.28 106.76 106.34 107.49 108.40 107.32 106.89 109.31
108.02 107.94 107.27 106.39 108.21 108.42 107.30 107.19 107.98 108.37
108.30 108.52 107.24 106.32 109.69 107.28 108.27 107.22 108.31 106.72
107.28 108.85 109.49 108.17 107.58 105.46 108.52 108.95 107.51 107.91
108.13 106.58 107.83 108.39 107.24 108.23 110.08 108.75 105.95 107.77
107.11 107.45 107.57 107.42 108.62 106.59 107.33 107.16 108.64 109.10
107.63 107.65 108.44 108.78 109.69 107.72 107.32 105.50 106.66 107.30

```

AVERAGE PERIOD = 0.10775E 03 RMS = 0.99889E 00 = 0.92708E 00 PERCENT

AVERAGE VELOCITY = 0.71019E 03 +/- 0.65840E 01

POPULATION DENSITIES

-4	-3	-2	-1	0	+1	+2	+3	+4
0.0000	0.1500	0.1750	0.4750	0.3500	0.3250	0.2500	0.1000	0.0750

80 DATA PTS 78 PTS UNDER CURVE = 0.97 PERCENT

Fig. 8 Computer Printout with Input Data Limited to $\pm 2\sigma$ of Mean

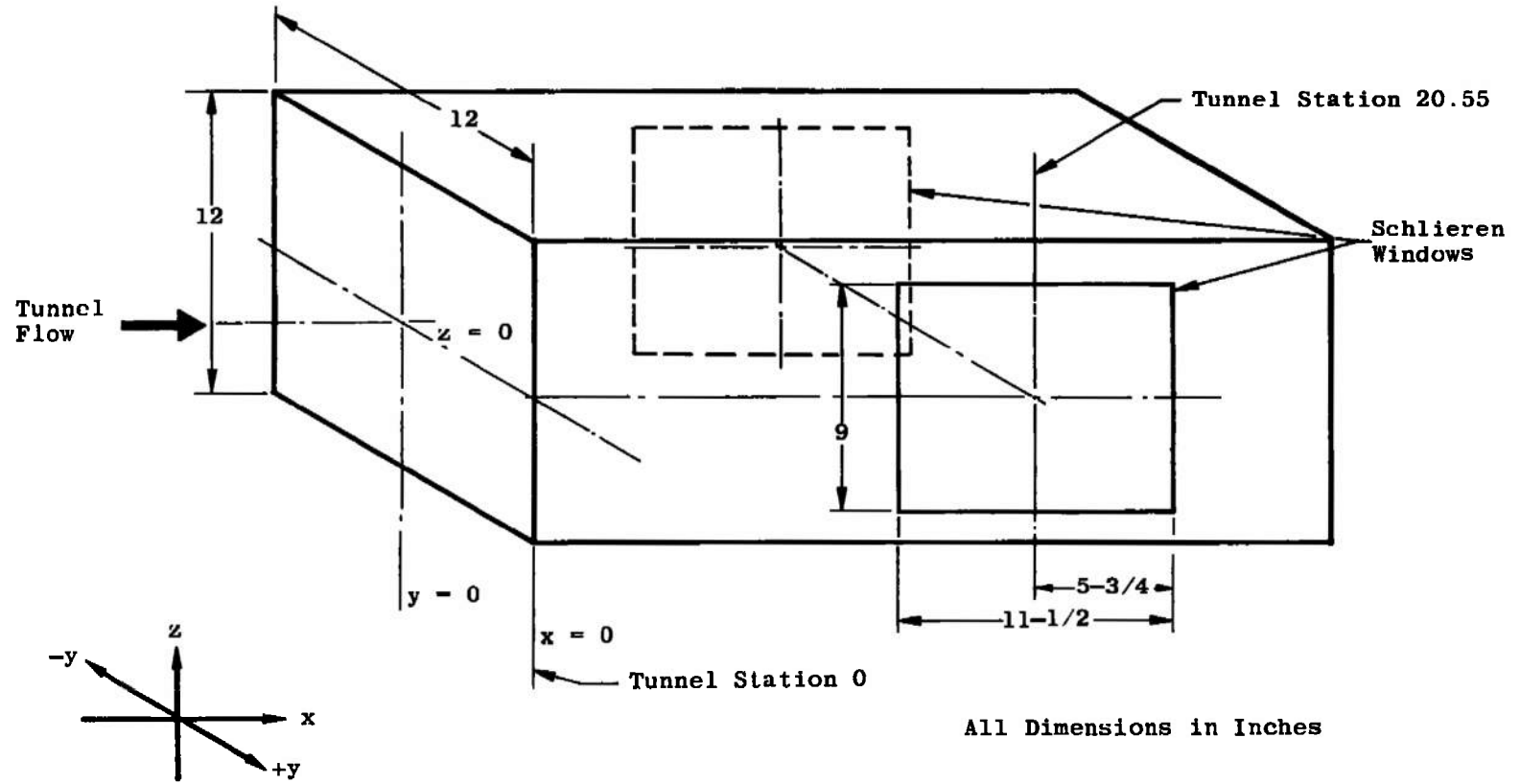


Fig. 9 Schematic of Test Section, PWT 1T Tunnel

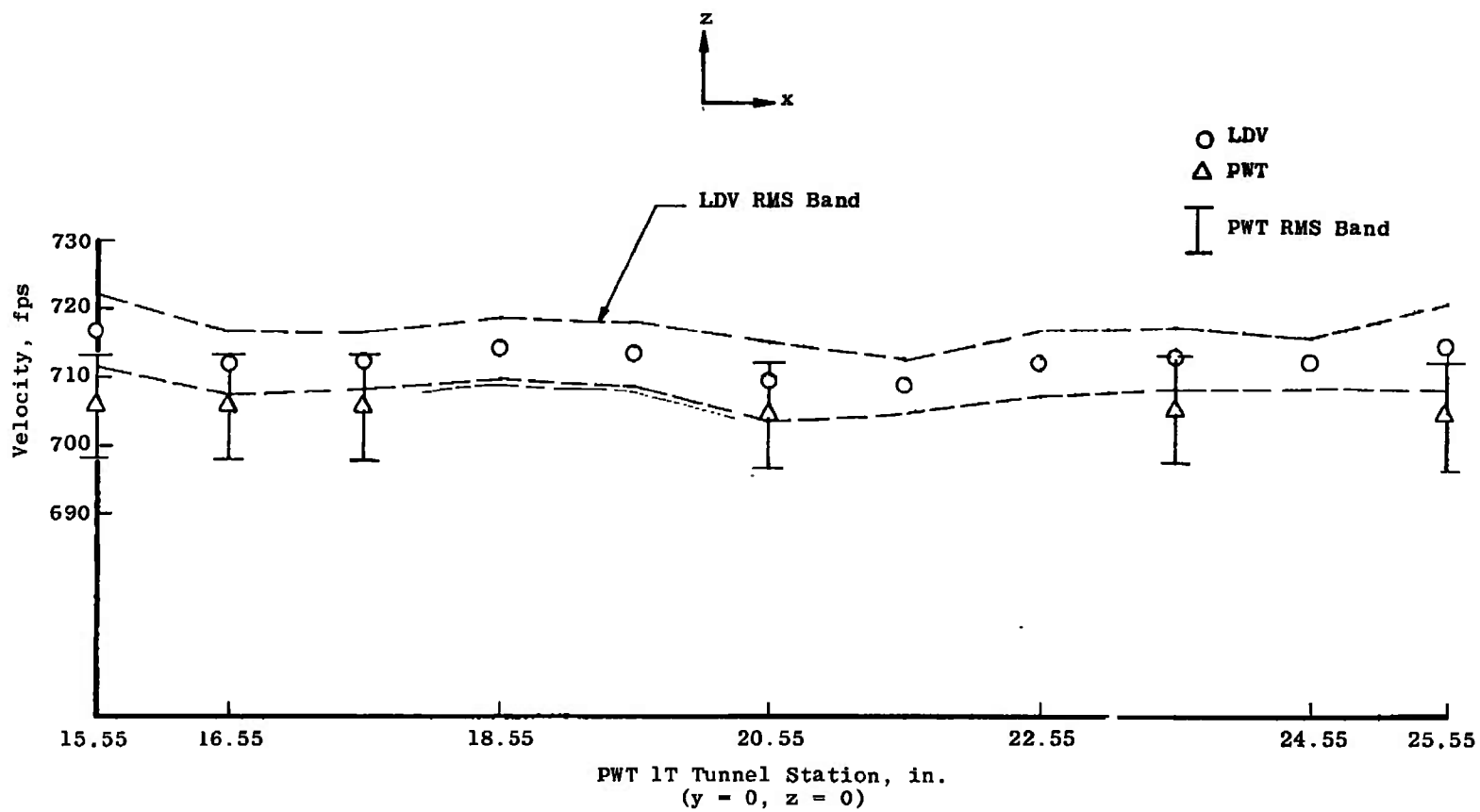


Fig. 10 Horizontal Velocity versus Axial Tunnel Position, $M = 0.6$

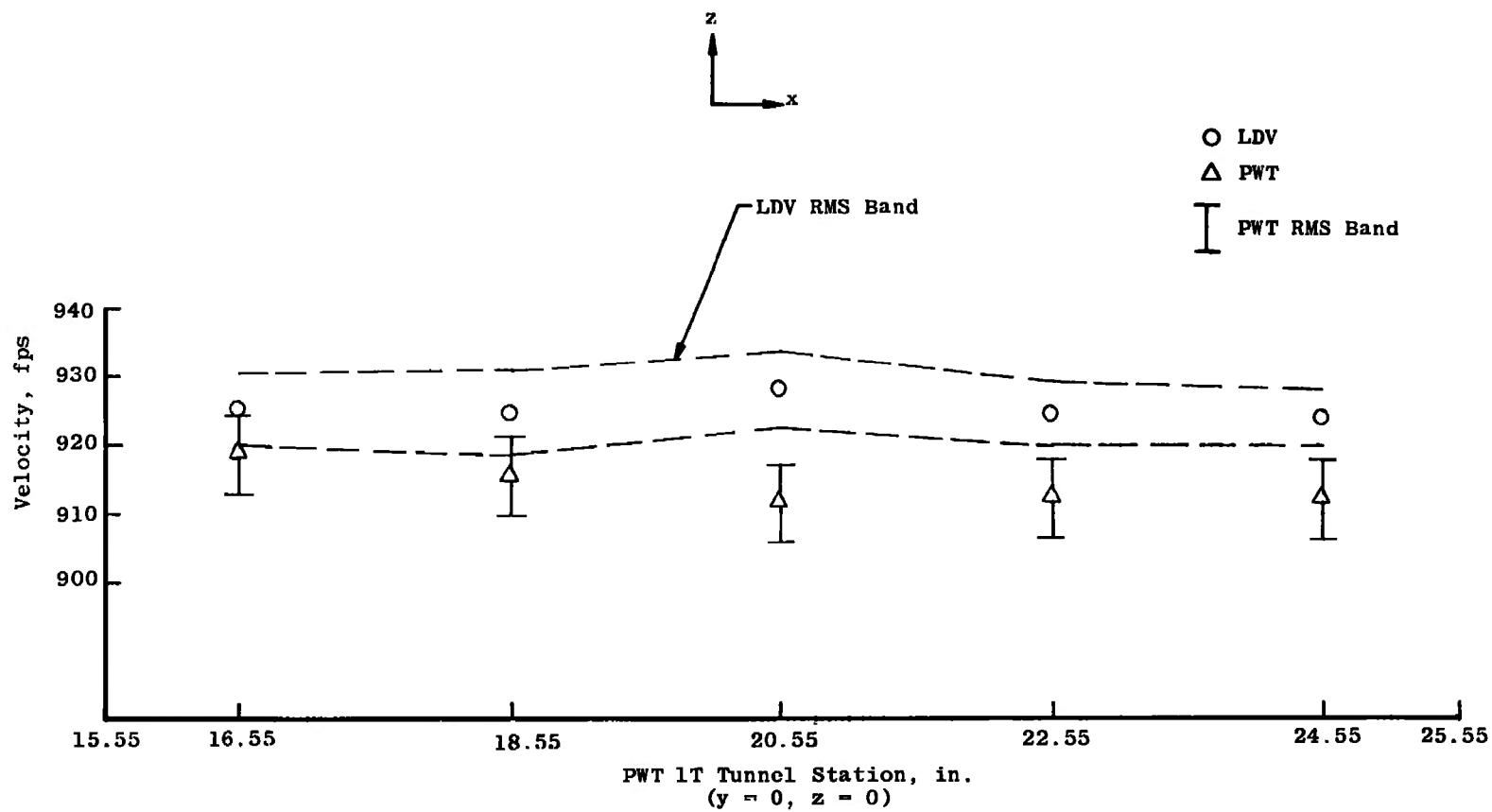


Fig. 11 Horizontal Velocity versus Axial Tunnel Position M = 0.8

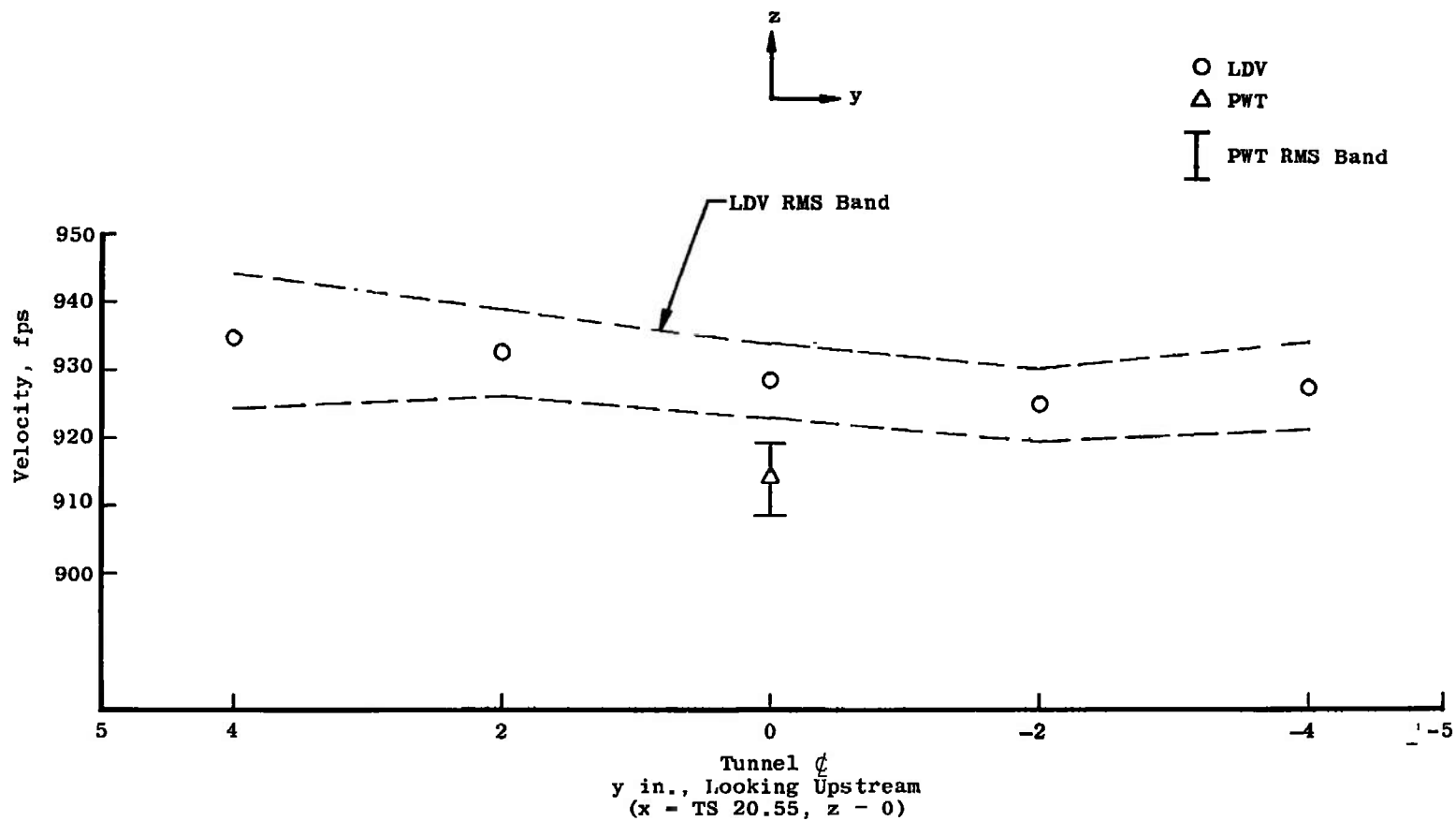


Fig. 12 Horizontal Velocity versus Transverse Position, $M = 0.8$

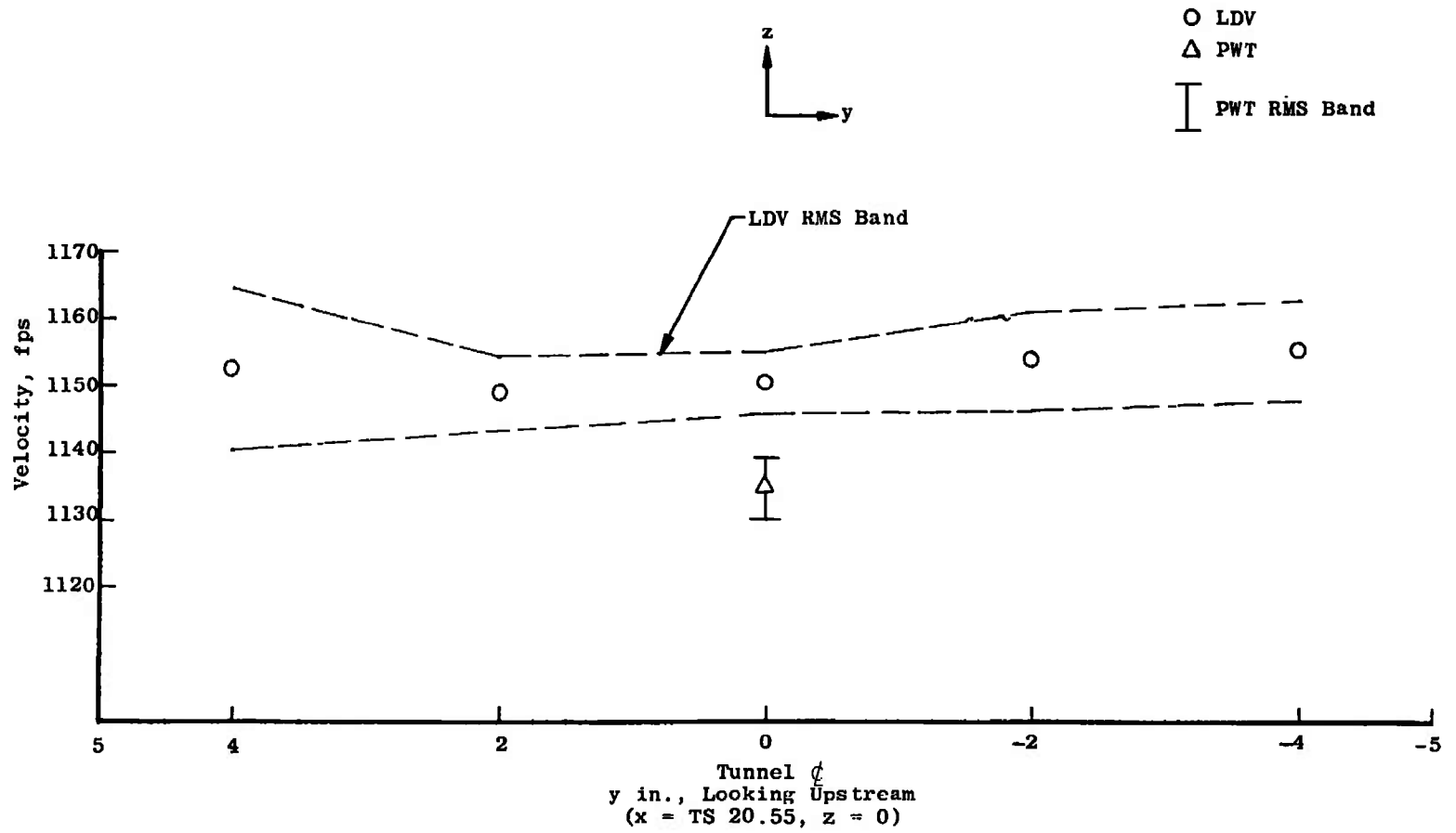


Fig. 13 Horizontal Velocity versus Transverse Position, $M = 1.0$

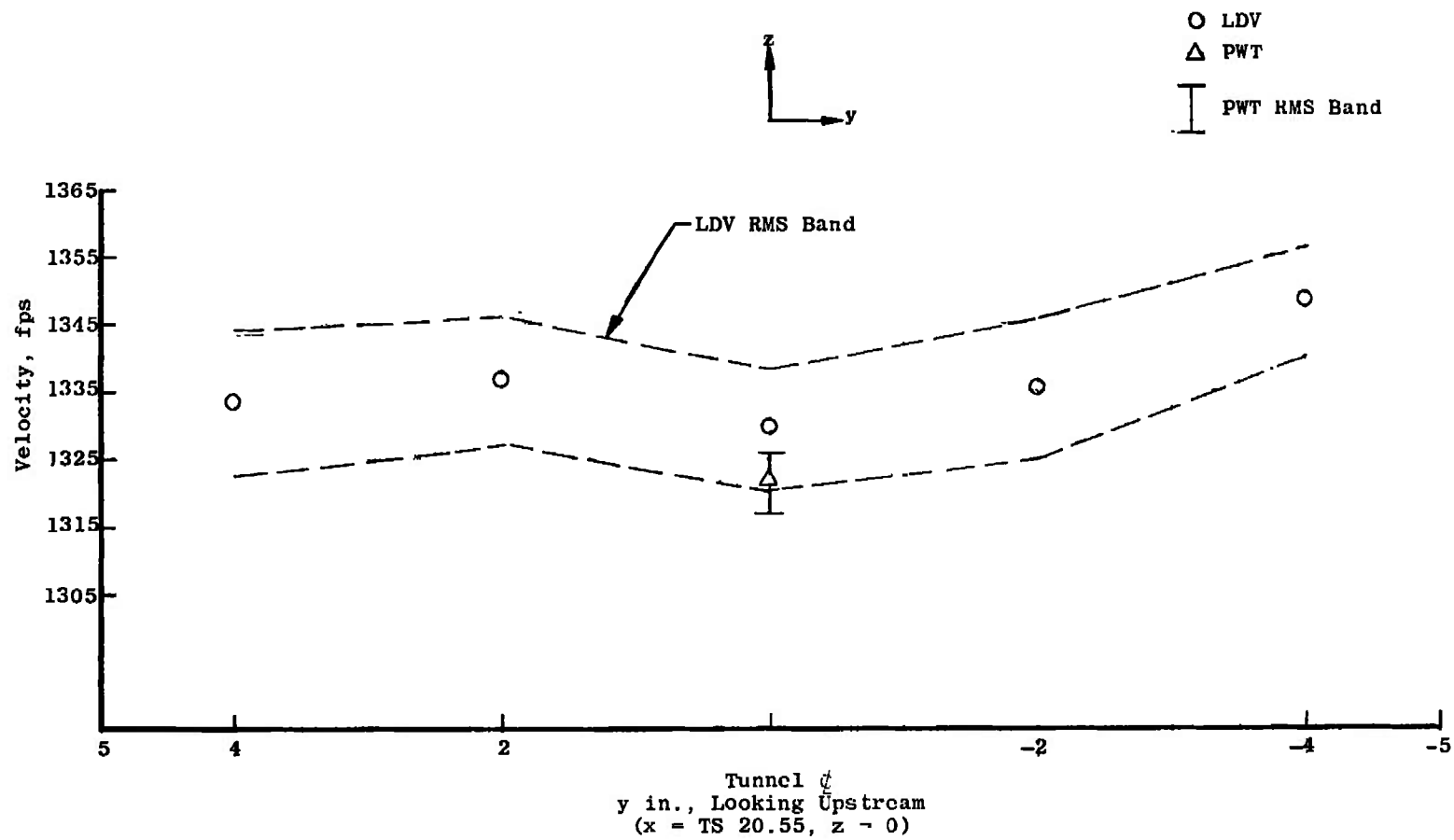
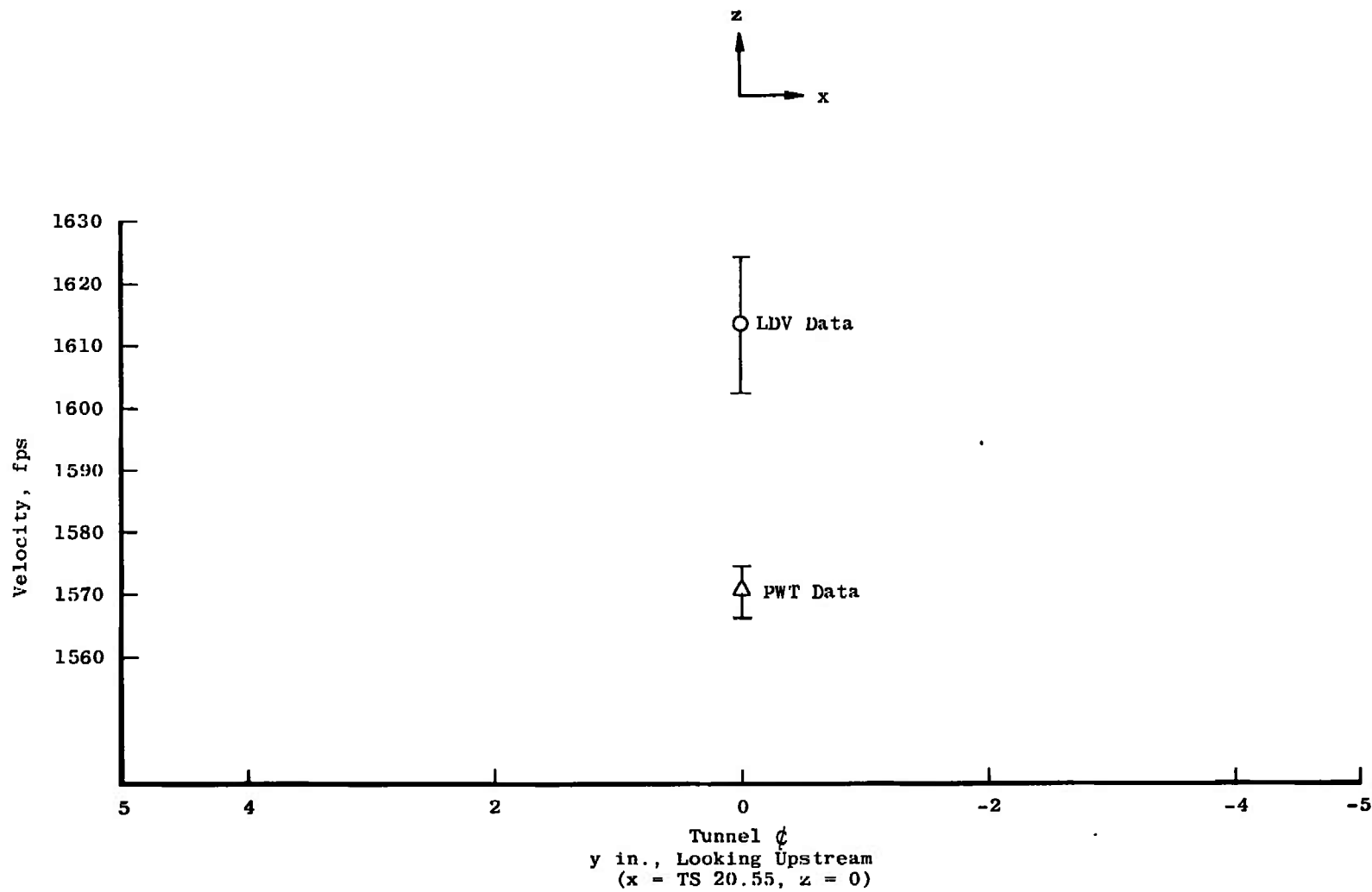


Fig. 14 Horizontal Velocity versus Transverse Position, $M = 1.2$

Fig. 15 Centerline Velocity, $M = 1.5$

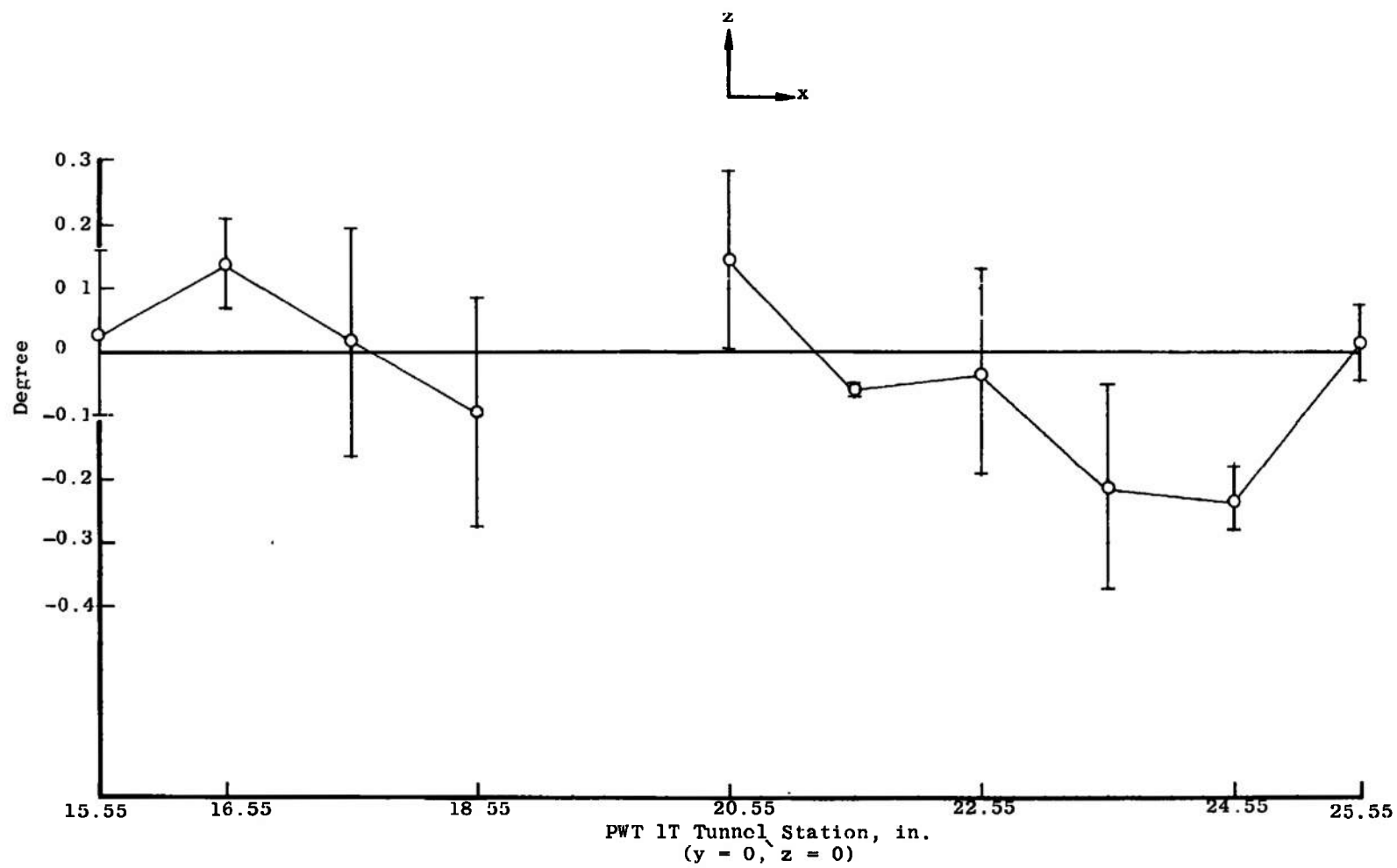


Fig. 16 Flow Angularity versus Axial Position, $M = 0.6$

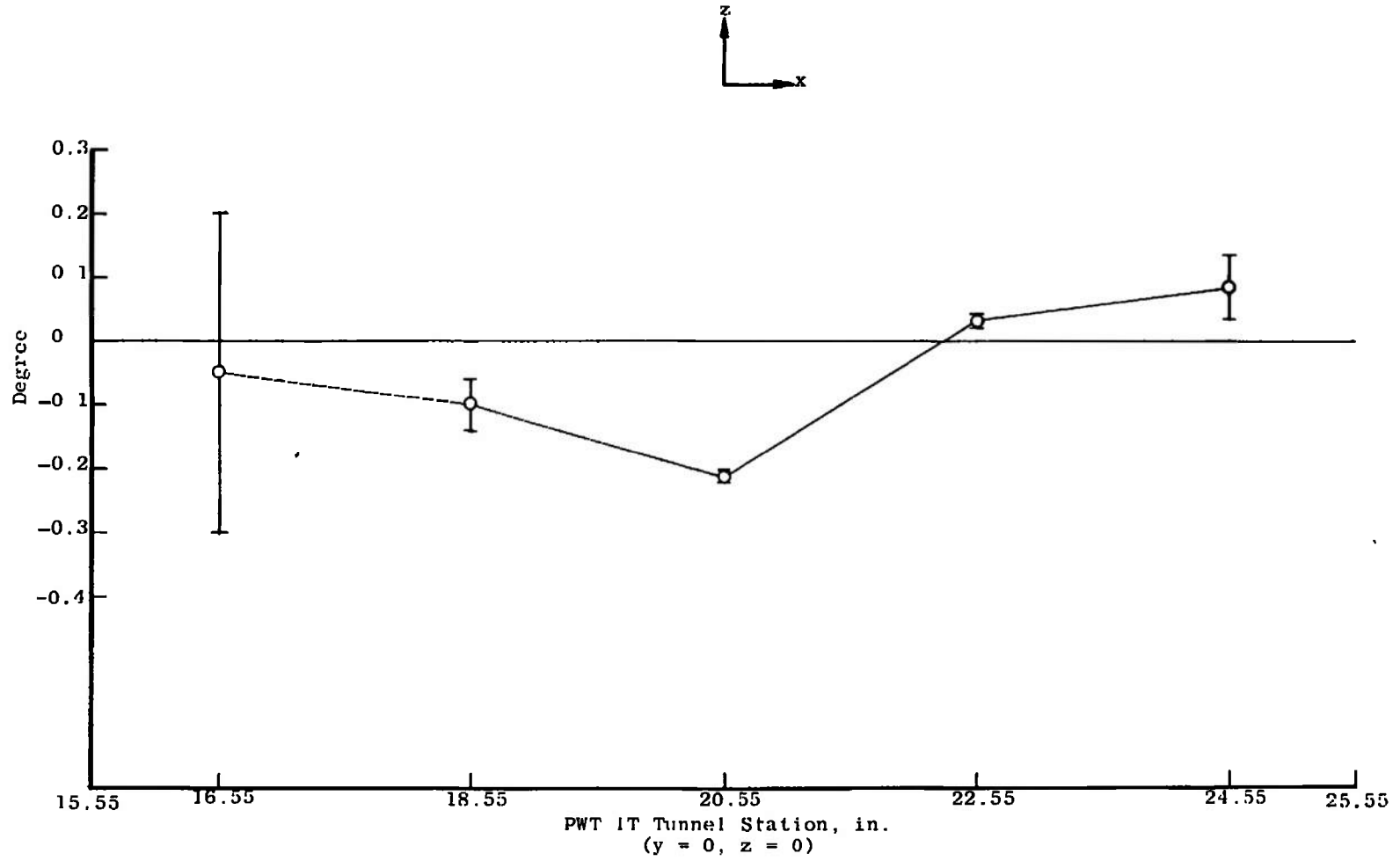


Fig. 17 Flow Angularity versus Axial Position, $M = 0.8$

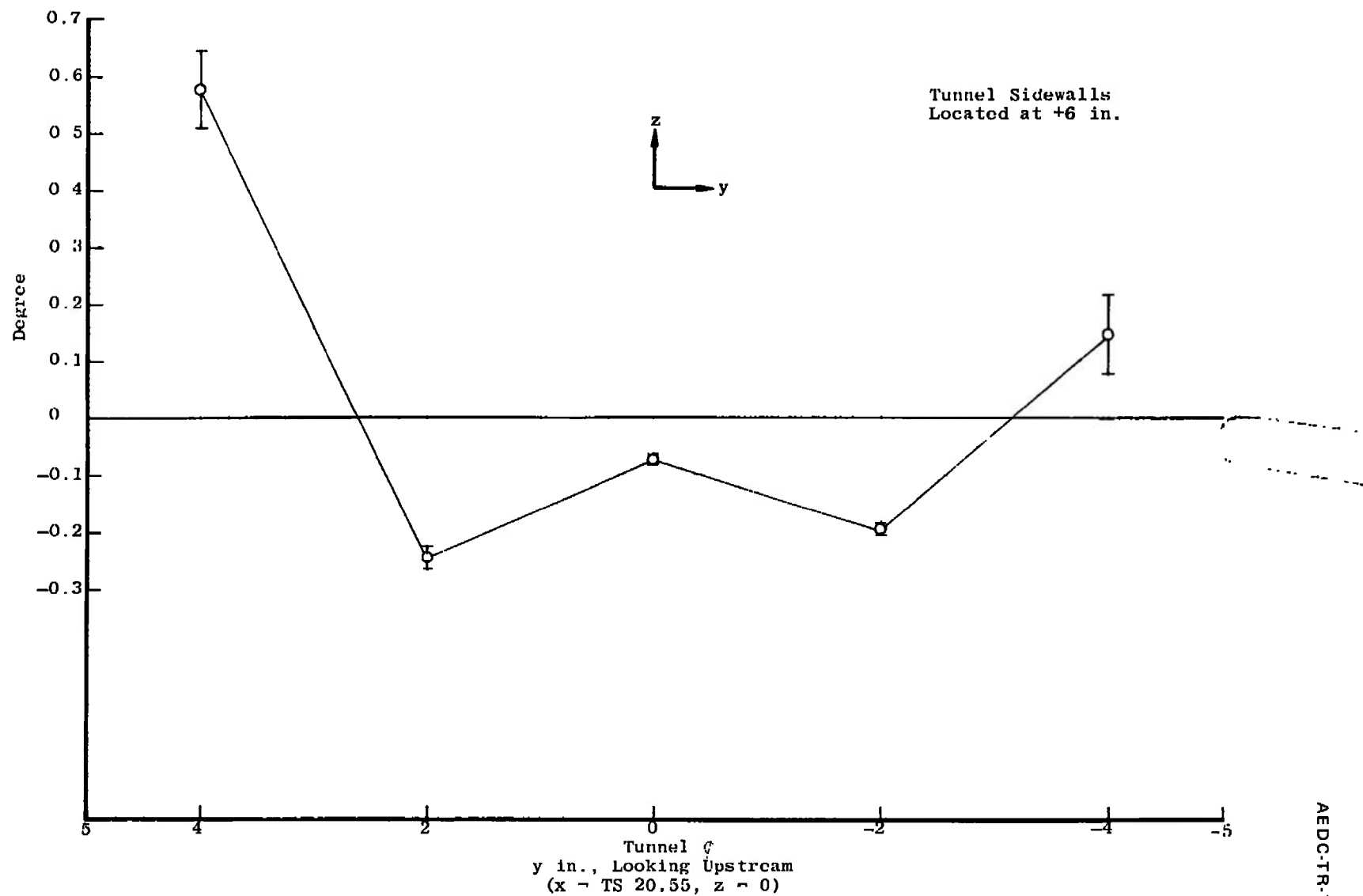


Fig. 18 Flow Angularity versus Transverse Position, $M = 0.8$

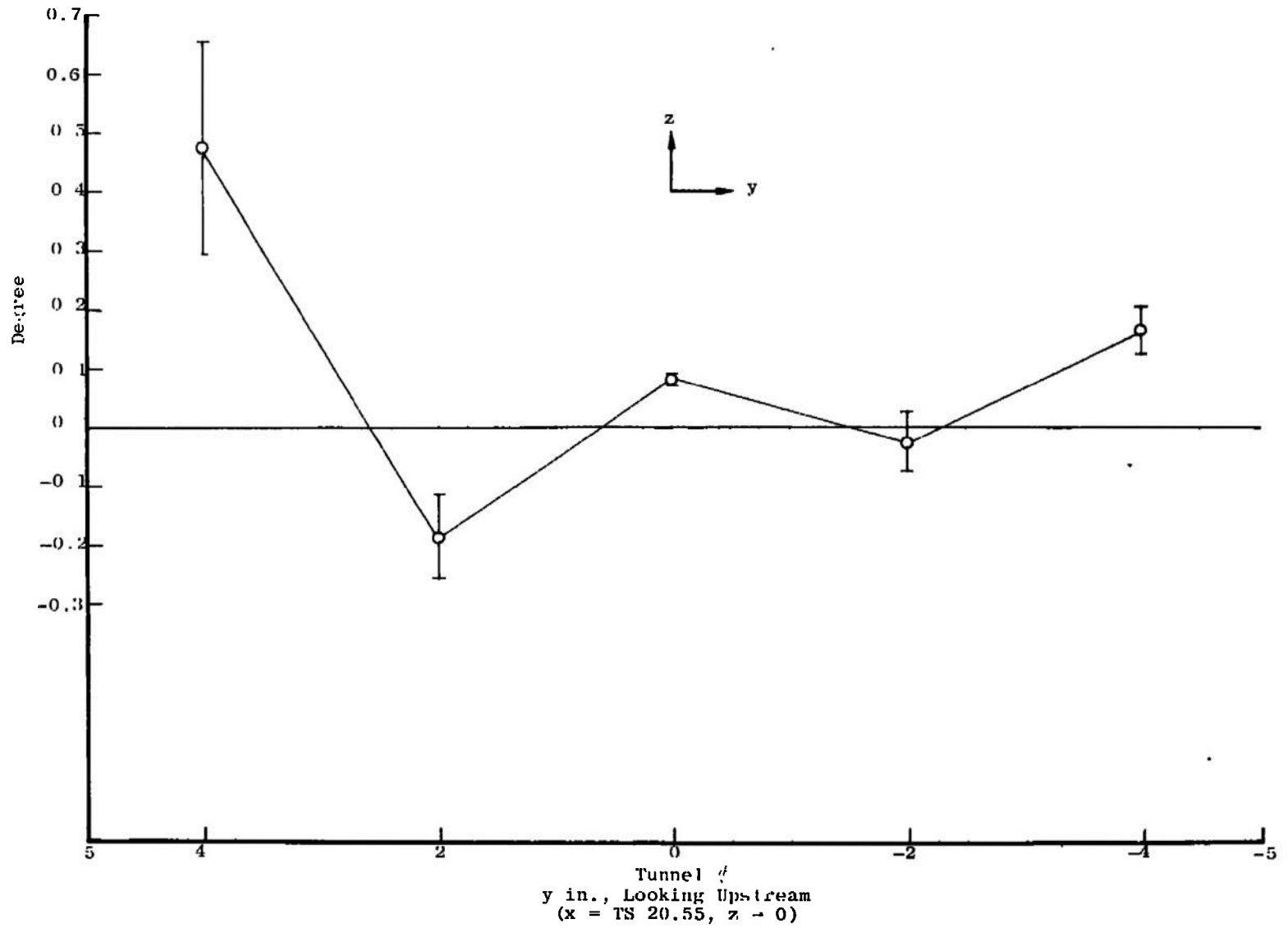


Fig. 19 Flow Angularity versus Transverse Position, $M = 1.0$

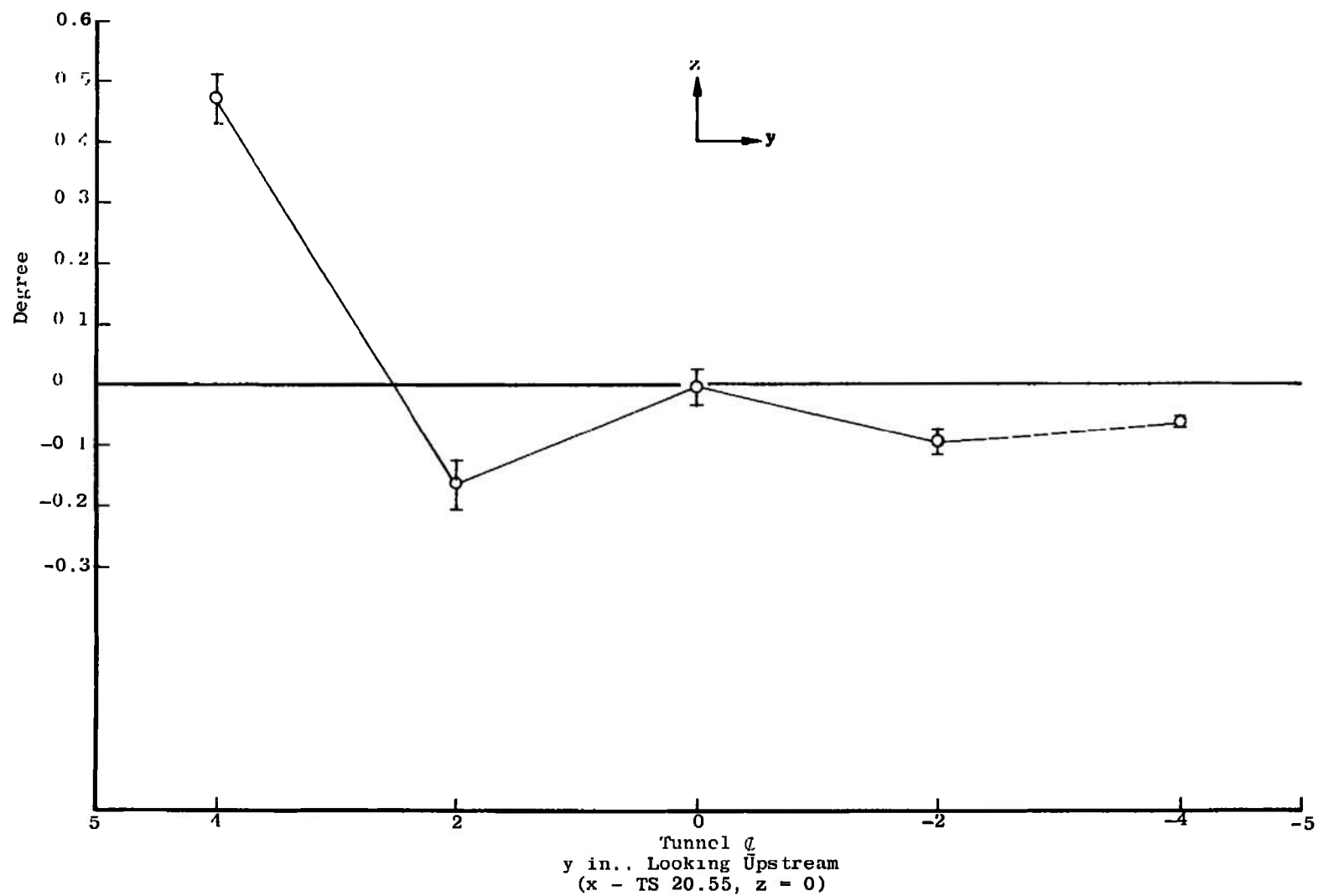


Fig. 20 Flow Angularity versus Transverse Position, $M = 1.2$

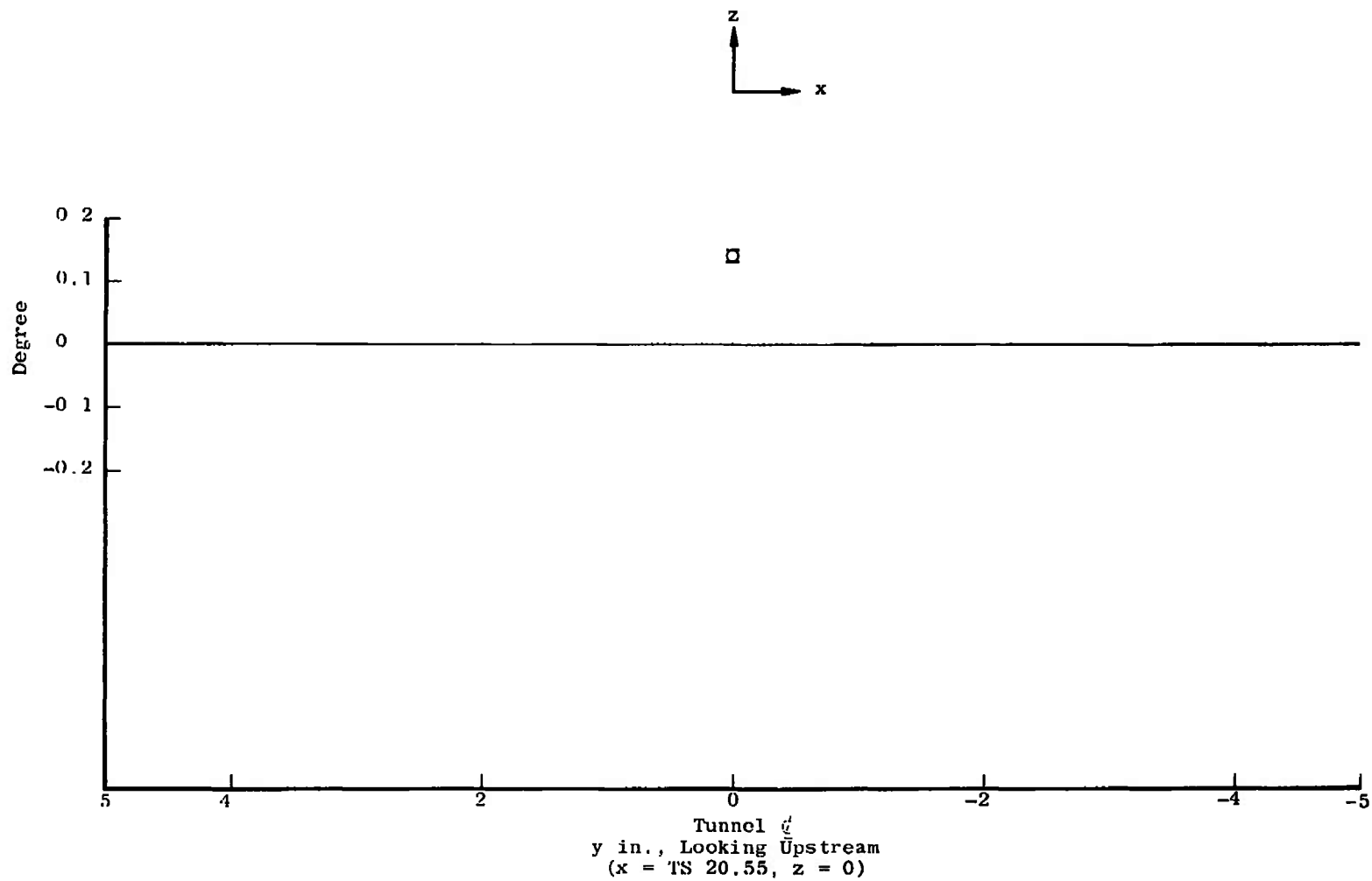


Fig. 21 Flow Angularity at Tunnel Centerline, $M = 1.5$

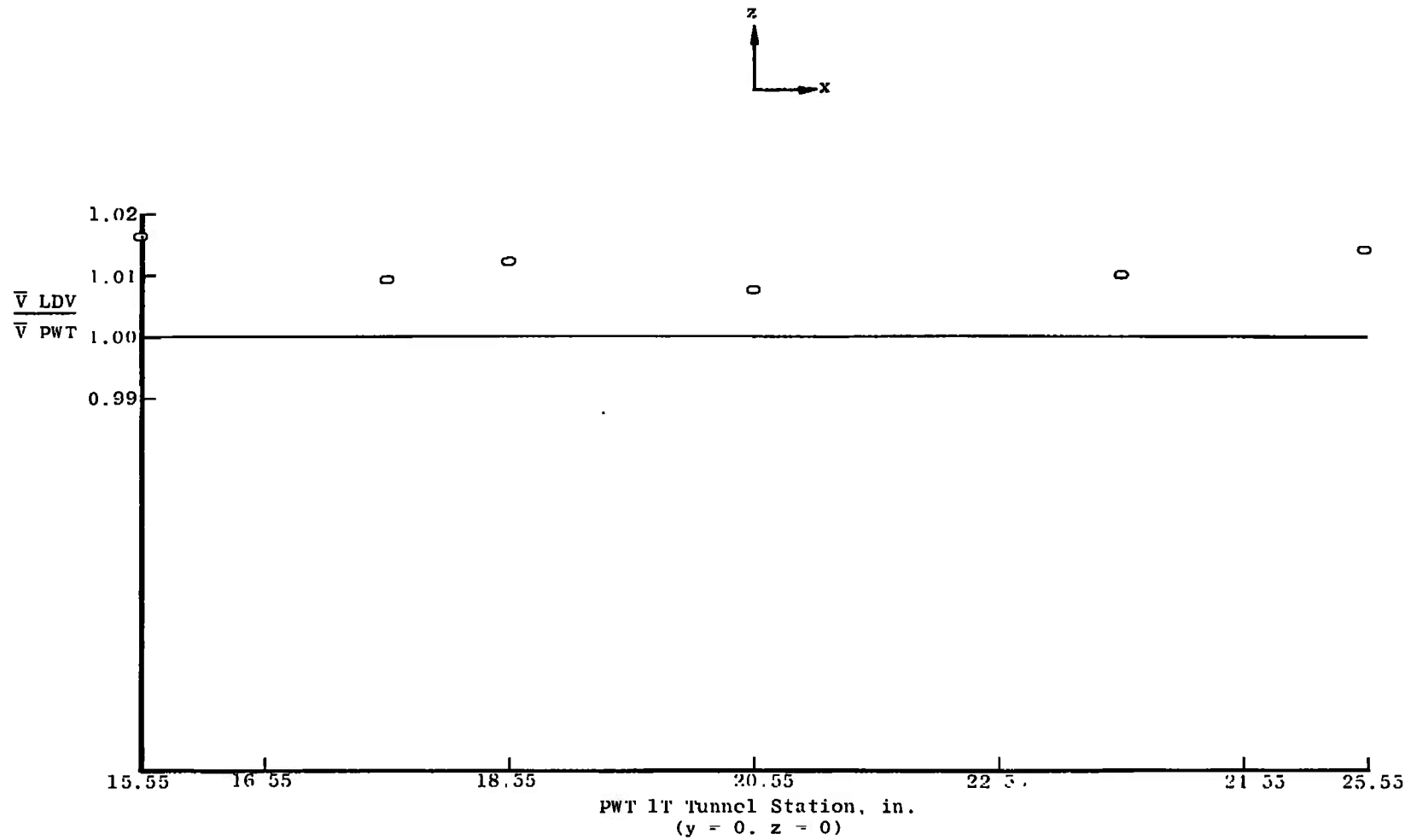


Fig. 22 Nondimensionalized Velocities versus Tunnel Position, $M = 0.6$

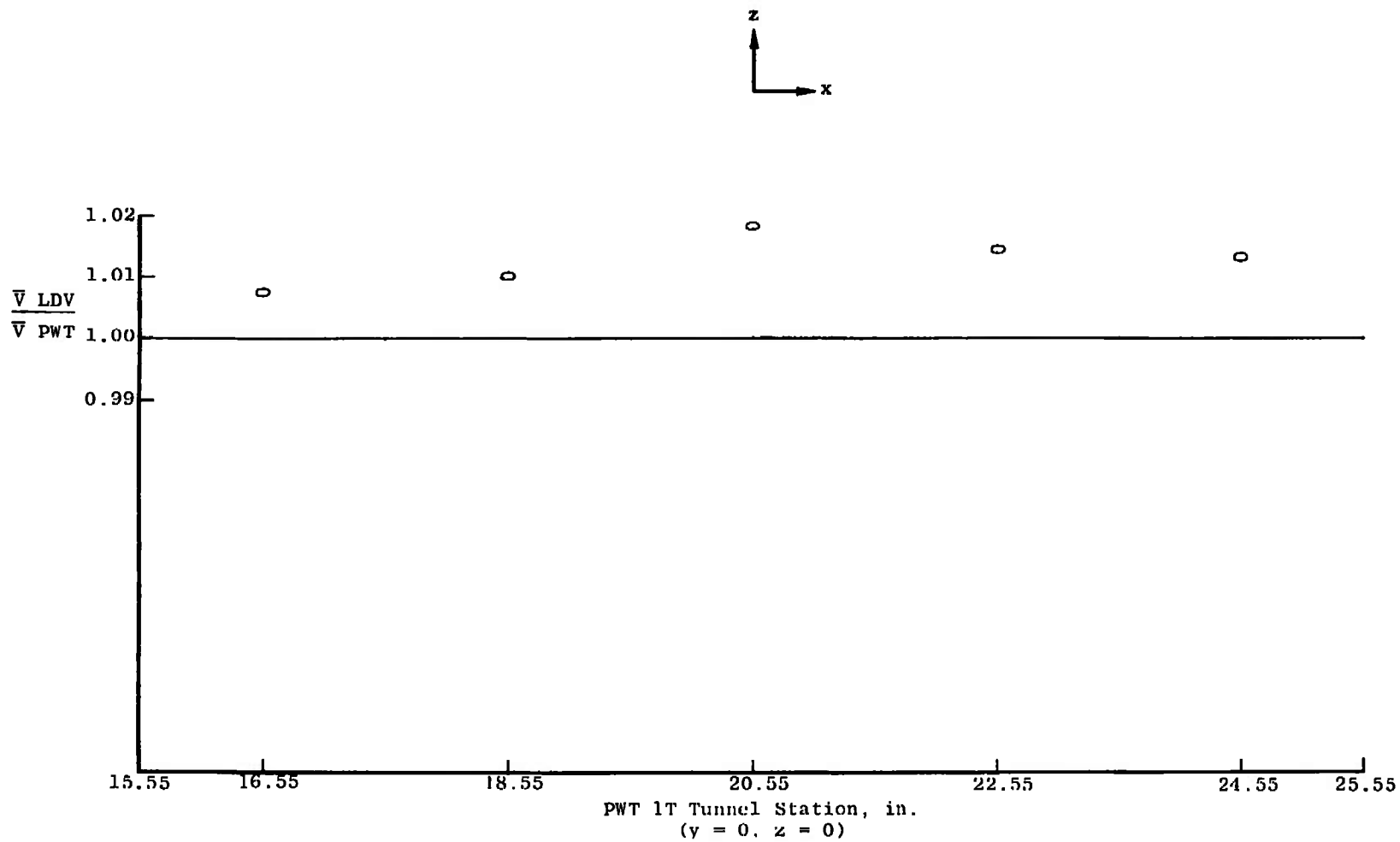


Fig. 23 Nondimensionalized Velocities versus Tunnel Position, and $M = 0.8$

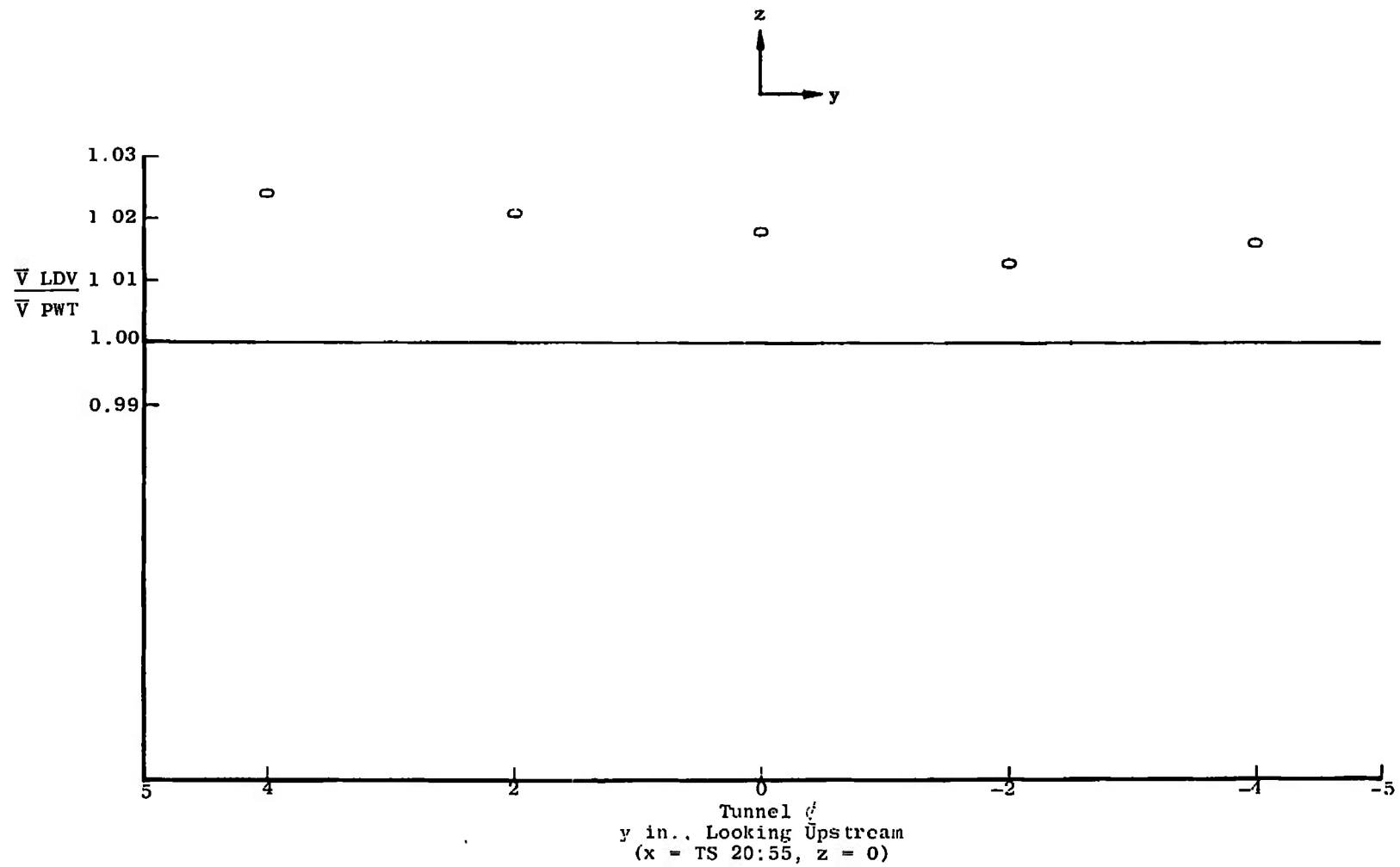


Fig. 24 Nondimensionalized Velocities versus Tunnel Position, $M = 0.8$

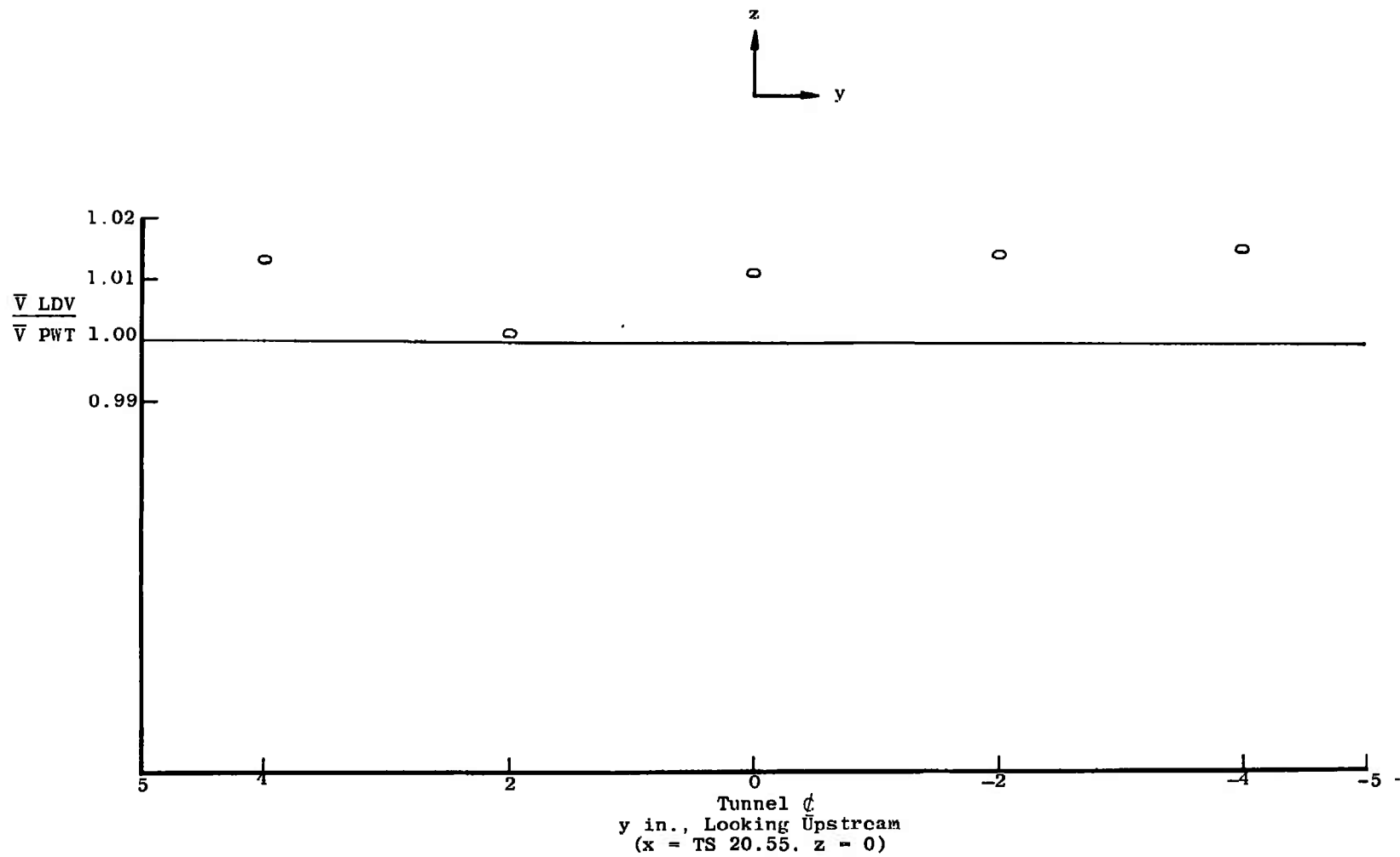


Fig. 25 Nondimensionalized Velocities versus Tunnel Position, $M = 1.0$

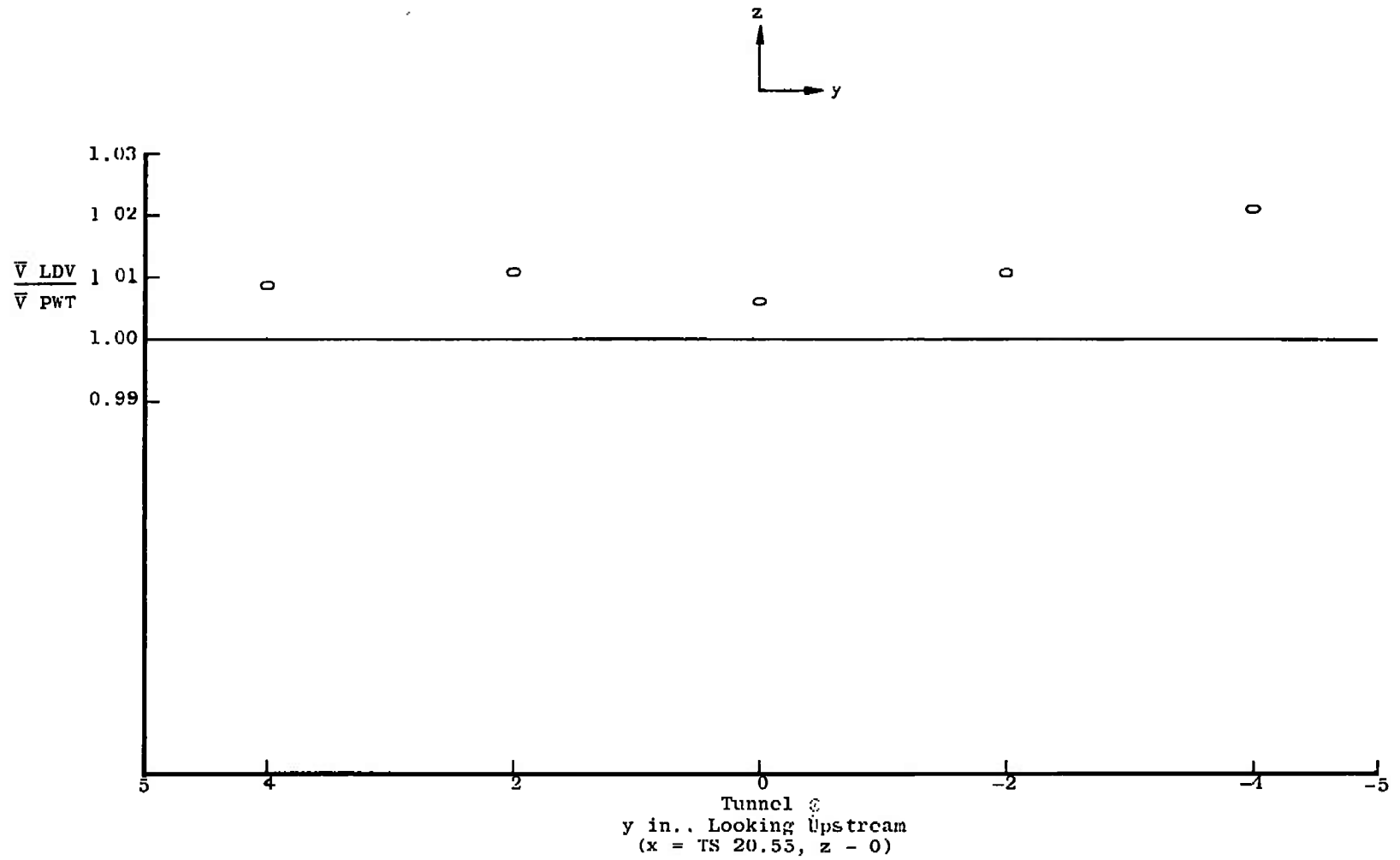


Fig. 26 Nondimensionalized Velocities versus Tunnel Position, $M = 1.2$

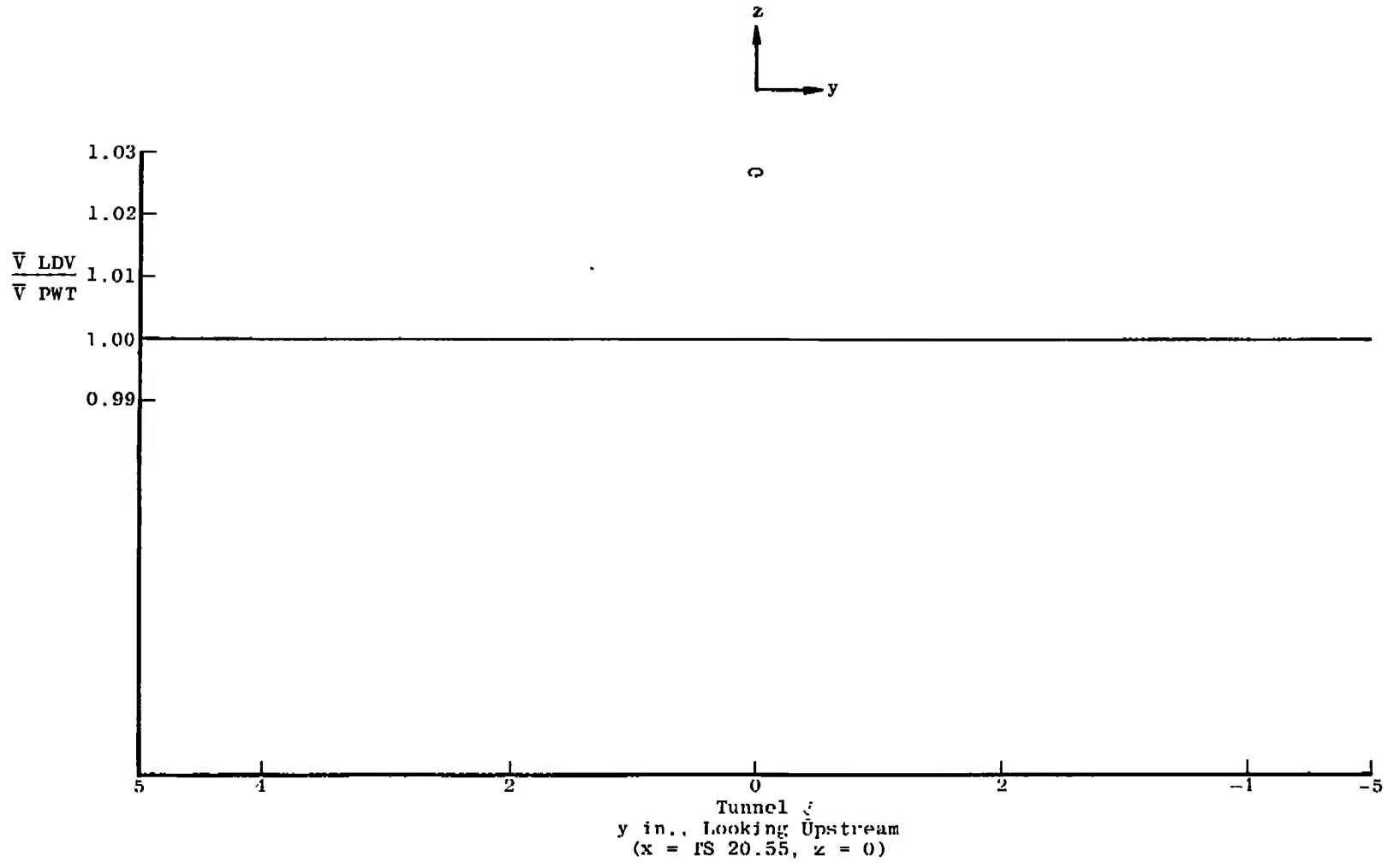


Fig. 27 Nondimensionalized Velocities versus Tunnel Position, $M = 1.5$

DOCUMENT CONTROL DATA - R & D

(Security classification of title, body of abstract and indexing annotation must be entered when the overall report is classified)

1 ORIGINATING ACTIVITY (Corporate author)		2a. REPORT SECURITY CLASSIFICATION	
Arnold Engineering Development Center Arnold Air Force Station, Tennessee		UNCLASSIFIED	
		2b. GROUP	
		N/A	
3 REPORT TITLE			
VELOCITY MEASUREMENTS IN AERODYNAMIC WIND TUNNEL (1T) USING A LASER DOPPLER VELOCIMETER			
4 DESCRIPTIVE NOTES (Type of report and inclusive dates)			
Final Report			
5 AUTHOR(S) (First name, middle initial, last name)			
F. H. Smith, A. E. Lennert, and J. O. Hornkohl, ARO, Inc.			
6 REPORT DATE		7a. TOTAL NO OF PAGES	7b. NO OF REFS
February 1972		44	6
8a. CONTRACT OR GRANT NO		9a. ORIGINATOR'S REPORT NUMBER(S)	
b. PROJECT NO		AEDC-TR-71-165	
c. Program Element 64719F		9b. OTHER REPORT NO(S) (Any other numbers that may be assigned this report)	
d.		ARO-OMD-TR-71-108	
10 DISTRIBUTION STATEMENT			
Approved for public release; distribution unlimited.			
11 SUPPLEMENTARY NOTES		12 SPONSORING MILITARY ACTIVITY	
Available in DDC		Arnold Engineering Development Center, Air Force Systems Command, Arnold AF Station, Tenn. 37389	
13 ABSTRACT			
<p>This report describes the application of a laser Doppler velocimeter (LDV) in a transonic wind tunnel. The LDV, an in-house-developed instrument, measured two velocity components using the dual scatter principle. The flow was not seeded for this test, and the output data was processed by a special data processor developed at AEDC. The velocity data and flow angularity are presented for five Mach numbers together with the velocities obtained using conventional wind-tunnel instrumentation.</p>			

KEY WORDS

velocity measurements
aerodynamic wind tunnel
laser velocimeters
doppler effect
transonic wind tunnel
fluid flows
photomultiplier tubes

LINK A

LINK B

LINK C

ROLE

WT

ROLE

WT

ROLE

WT